

The Relationship between Lower Stratospheric Ozone in the Southern High Latitudes and Sea Surface Temperature in the East Asian Marginal Seas in Austral Spring

Wenshou Tian¹, Yuanpu Li¹, Fei Xie^{2*}, Jiankai Zhang¹, Martyn P. Chipperfield³,
Wuhu Feng⁴, Yongyun Hu⁵, Sen Zhao^{6,7}, Xin Zhou⁸, Yun Yang², Xuan Ma²

¹*College of Atmospheric Sciences, Lanzhou University, Lanzhou, China*

²*College of Global Change and Earth System Science, Beijing Normal University, Beijing, China*

³*ICAS, School of Earth and Environment, University of Leeds, Leeds, UK*

⁴*NCAS, School of Earth and Environment, University of Leeds, Leeds, UK*

⁵*Department of Atmospheric and Oceanic Sciences, School of Physics, Peking University, Beijing, China*

⁶*Key Laboratory of Meteorological Disaster of Ministry of Education, and College of Atmospheric Science, Nanjing University of Information Science and Technology, Nanjing, China*

⁷*School of Ocean and Earth Science and Technology, University of Hawaii at Mānoa, Honolulu, Hawaii*

⁸*Plateau Atmosphere and Environment Key Laboratory of Sichuan Province, College of Atmospheric Science, Chengdu University of Information Technology, Chengdu, China*

Submitted as an Article to: ***Atmospheric Chemistry and Physics***

*Corresponding author:

Dr. Fei Xie, Email: xiefei@bnu.edu.cn.

1 **Abstract**

2 Using satellite observations, reanalysis data, and model simulations, this study
3 investigates the effect of sea surface temperatures (SST) on interannual variations of
4 lower stratospheric ozone in the southern high latitudes in austral spring. It is found
5 that the SST variations across the East Asian Marginal Seas (5 °S–35 °N, 100 °E–140 °E)
6 rather than the tropical eastern Pacific Ocean, where ENSO occurs, have the most
7 significant correlation with the southern high latitude lower stratospheric ozone
8 changes in austral spring. Further analysis reveals that planetary waves originating
9 over the marginal seas in austral spring can propagate towards to southern middle to
10 high latitudes via teleconnection pathway. The anomalous propagation and dissipation
11 of ultra-long Rossby waves in the stratosphere strengthen/cool (weaken/warm) the
12 southern polar vortex which produces more (less) active chlorine and enhances
13 (suppresses) ozone depletion in the southern high latitude stratosphere on one hand,
14 and impedes (favors) the transport of ozone from the southern middle latitude
15 stratosphere to high latitude on the other. The model simulations also reveal that
16 approximately 17% of the decreasing trend in the southern high latitude lower
17 stratospheric ozone observed over the past five decades may be associated with the
18 increasing trend in SST over the East Asian Marginal Seas.

1. Introduction

Ozone variations over recent decades exhibit not only strong trends, forced by changes in ozone-depleting substances superimposed on a changing climate, but also interannual variability influenced by various external and internal climate forcings (e.g. Manney et al. 1994; Müller et al., 1994, 2005; Weiss et al., 2001; Hadjinicolaou et al., 2002; Tian and Chipperfield, 2005; Austin et al., 2006, 2010; Eyring et al., 2010; Liu et al., 2011, 2013; Douglass et al., 2014). Ozone variations can change the amount of harmful solar ultraviolet rays reaching the Earth's surface (Kerr and McElroy, 1993) and even influence climate (Forster and Shine, 1997; Thompson et al., 2011; Li et al., 2016; Xie et al., 2016). Therefore, clarifying the processes that are responsible for ozone variability is crucial for understanding how global climate interacts with ozone variations (Austin et al., 2006; Hess and Lamarque, 2007; Frossard et al., 2013; Rieder et al., 2013). Many previous studies have analyzed the ozone variability caused by external processes such as volcanic aerosols (e.g. Hofmann and Oltmans, 1993; Rozanov et al., 2002; Dhomse et al., 2015) and the solar cycle (e.g. Chandra and McPeters, 1994; Rozanov et al., 2005; Dhomse et al., 2016) and these studies showed that volcanic aerosols and solar variations can result in considerable short- and long-term variations in ozone levels. Ozone variations can also be caused by changes in the surface climate (Zhang et al., 2014). Other studies have reported the effects of internal climate variability on ozone, including El Niño–Southern Oscillation (ENSO; Ziemke and Chandra, 1999; Cagnazzo et al., 2009; Randel et al., 2009; Xie et al., 2014a, 2014b; Zhang et al., 2015a, 2015b), Madden–Julian Oscillation (MJO; Fujiwara et al., 1998; Tian et al., 2007; Liu et al., 2009; Weare, 2010; Li et al., 2012), Arctic Oscillation (AO) or North Atlantic Oscillation (NAO; Schnadt and Dameris, 2003; Lamarque and Hess, 2004; Creilson et al., 2005;

1 Steinbrecht et al., 2011), and Quasi-Biennial Oscillation (QBO; Bowman, 1989; Tung
2 and Yang, 1994; Dhomse, 2006; Li and Tung, 2014). These studies indicate that ozone
3 over different regions shows different variability due to the location-specific nature of
4 the processes that influence this variability.

5 The stratospheric ozone hole in austral spring (Farman et al., 1985) over the
6 Antarctic has been shown to have an important impact on the Southern Hemisphere
7 climate (Shindell and Schmidt, 2004; Son et al., 2008, 2009, 2010, Perlwitz et al.,
8 2008; Feldstein, 2011, Kang et al., 2011, Polvani et al., 2011; Thompson et al., 2011;
9 Cagnazzo et al., 2013; Keeble et al., 2014; Previdi and Polvani, 2014). Although the
10 principal mechanisms responsible for the formation of the ozone hole are well
11 understood (e.g., Solomon, 1990, 1999; Ravishankara et al., 1994, 2009), the factors
12 or processes that generate interannual variations in ozone levels in the southern high
13 latitude stratosphere remain under debate. Among various factors, the QBO has been
14 reported to have a significant impact on the interannual variations of the Antarctic
15 ozone (Garcia and Solomon, 1987; Lait et al., 1989; Mancini et al., 1991; Gray and
16 Ruth, 1993; Bodeker and Scourfield, 1995; Shindell et al., 1997a). The September to
17 March levels of ozone over the Antarctic is also marginally correlated with the
18 wintertime mean eddy heat flux (Weber et al., 2003). Heat transport induced by
19 upward propagating planetary waves warms the polar vortex (Schoeberl and
20 Hartmann, 1991), which reduces the occurrence of polar stratospheric clouds (PSCs),
21 a key prerequisite for the heterogeneous chemistry that depletes Antarctic ozone.
22 Subsequent efforts to understand Antarctic ozone variations during individual years
23 have considered planetary wave activity, which account for much of the interannual
24 variations of ozone levels over the Northern Hemisphere (Hadjinicolaou et al., 1997;
25 Fusco and Salby, 1999; Salby and Callaghan, 2004, 2007a, 2007b; Hadjinicolaou and

1 Pyle, 2004). Studies based on measurements (Bodeker and Scourfield, 1995),
2 modeling (Shindell et al., 1997a, 1997b), and reanalysis data (Huck et al., 2005) have
3 shown that interannual differences in the severity of Antarctic ozone depletion are
4 anti-correlated with Southern Hemisphere planetary wave activity. However, the
5 source of the planetary wave activity that modulates interannual variability in
6 southern high latitude stratospheric ozone is still not well understood.

7 Variations in tropical sea surface temperatures (SST) associated with El
8 Niño-Southern Oscillation (ENSO), are an important factor in the modulation of the
9 planetary wave activity in the Northern Hemisphere that affects the interannual
10 variability of temperature and ozone levels in the northern polar stratosphere (Sassi et
11 al., 2004; Manzini et al., 2006; Calvo et al., 2004, 2009; Cagnazzo et al., 2009; Hu
12 and Pan, 2009; Hurwitz et al., 2011a, b; Ren et al., 2010; Zubiaurre and Calvo, 2012;
13 Xie et al., 2012; Yao et al., 2015). The long-term trend in tropical SST also has a
14 correspondence to the trend of temperature in the southern polar stratosphere (Grassi
15 et al., 2005, 2006; Hu and Fu, 2009; Li et al., 2010; Clem et al., 2016). Although
16 ENSO is reported to cause circulation and temperature anomalies in the southern high
17 latitude stratosphere, the interannual variability of the southern polar vortex and ozone
18 levels over the past three decades cannot be explained by ENSO variations alone
19 (Angell, 1988, 1990; Hurwitz et al., 2011a, 2011b; Lin et al., 2012; Wilson et al., 2014;
20 Evtushevsky et al., 2015; Yu et al., 2015; Yang et al., 2015; Welhouse et al., 2016).

21 Over recent decades, SST in the East Asian Marginal Seas has exhibited an
22 increasing trend with strong interannual variations (Zheng et al., 2014). Zhao et al.
23 (2015, 2016) pointed out that Rossby waves generated by variations in the SST of the
24 South China Sea can cross the equator and propagate towards to southern middle to
25 high latitudes in austral spring. It is likely that the Rossby waves generated by SST

1 changes in austral spring in the vicinity of the East Asian Marginal Seas can cross the
2 equator to the Southern Hemisphere and regulate austral spring ozone levels in the
3 southern high latitude stratosphere via their influence on the southern stratospheric
4 circulation. Therefore, it is worthwhile to examine the potential connections between
5 SST variations over the East Asian Marginal Seas and southern high latitude lower
6 stratospheric ozone variations. The remainder of the paper is organized as follows.
7 The data, method and model used are introduced and briefly described in section 2.
8 Section 3 analyzes the connection between the East Asian Marginal Seas and southern
9 high latitude lower stratospheric ozone. Section 4 presents and discusses the
10 simulations of the connection. Finally, the results are summarized and conclusions
11 drawn in section 5.

12

13 **2. Data, Model, and Methods**

14 The ozone data used in this study is obtained from the NASA Modern Era
15 Retrospective Analysis for Research and Applications (MERRA) dataset version 2
16 (Rienecker et al., 2011), TOMCAT/SLIMCAT 3-D model simulations (Chipperfield,
17 2006), Global OZone Chemistry And Related trace gas Data records for the
18 Stratosphere (GOZCARDS) ozone satellite data (Froidevaux et al. 2015) and The
19 Stratospheric Water and OzOne Satellite Homogenized (SWOOSH) ozone satellite
20 data (Davis et al. 2016). The MERRA2 data (1979–2015) ($\text{lon} \times \text{lat}$: $1.25^\circ \times 1.25^\circ$)
21 has 42 pressure levels from the surface up to 0.1 hPa. The vertical resolution of
22 MERRA2 is ~1–2 km in the UTLS and 2–4 km in the middle and upper stratosphere.
23 MERRA2 is assimilated by the Goddard Earth Observing System Model, Version 5
24 (GEOS-5) with ozone from the Solar Backscattered Ultra Violet (SBUV) radiometers
25 from October 1978 to October 2004, and thereafter from the Ozone Monitoring

1 Instrument (OMI) and AURA Microwave Limb Sounder (MLS) (Bosilovich et al.,
2 2015). The MERRA2 reanalysis ozone data compares well with satellite ozone
3 observations (Wargan et al., 2017) and shows a better representation of the QBO and
4 stratospheric ozone compared to MERRA1 (Coy et al., 2016). In the present study, the
5 ozone field ($\text{lon} \times \text{lat}$: $5.625^\circ \times 5.5^\circ$) simulated by a 3D offline chemical transport
6 model, SLIMCAT (1979–2015) (Feng et al., 2007, 2011), is also used. The simulation
7 performed in this study is driven by horizontal winds and temperatures from
8 meteorological analyses of the ERA-Interim data provided by European Centre for
9 Medium-Range Weather Forecasts (ECMWF) (Dee et al., 2011). The vertical
10 advection in the model is calculated from the divergence of the horizontal mass flux
11 (Chipperfield, 2006), and chemical tracers are advected by the conservation of
12 second-order moments (Prather, 1986). The zonal mean satellite-based GOZCARDS
13 (1979–2012) is produced from high quality data from past missions (e.g., SAGE,
14 HALOE data) as well as ongoing missions (ACE-FTS and Aura MLS). Its meridional
15 resolution is 10° with 25 pressure levels from the surface up to 0.1 hPa. The zonal
16 mean SWOOSH dataset (1984–2015) is a merged record of stratospheric ozone and
17 water vapor measurements taken by a number of limb sounding and solar occultation
18 satellites (SAGE-II/III, UARS HALOE, UARS MLS, and Aura MLS instruments). Its
19 meridional resolution is 2.5° with 31 pressure levels from 300 to 1 hPa.

20 Figure 1 shows the time series of original ozone concentrations in austral spring
21 averaged over the region 200–50 hPa and 60–90 °S for MERRA2 and SLIMCAT
22 ozone datasets and over the region 200–50 hPa and 60–75 °S for GOZCARDS and
23 SWOOSH ozone datasets (satellite datasets have no or very limited coverage in the
24 southern polar region), where the variability and trend of ozone concentration is most
25 pronounced in the Southern Hemisphere (Austin and Wilson, 2006; Solomon 1990,

1999; Ravishankara et al., 1994, 2009), from the four datasets. We can see the original ozone concentrations from MEERA2 and SLIMCAT are somewhat lower than that from the GOZCARDS and SWOOSH (Fig. 1a); however, the variabilities of ozone concentrations from these four datasets are similar (Fig. 1b).

SST is obtained from HadISST dataset compiled by the UK Met Office Hadley Centre for Climate Prediction and Research (Rayner et al., 2003). Geopotential height, zonal wind, and temperature fields are obtained from the ECMWF ERA-Interim dataset.

We also use version 4 of the Whole Atmosphere Community Climate Model (WACCM4) in this study since WACCM has been shown to have a good performance in simulating the stratospheric circulation, temperature and ozone variations (Garcia et al. 2007). WACCM4 is part of the Community Earth System Model (CESM) framework developed by the National Center for Atmospheric Research (NCAR). WACCM4 uses a finite-volume dynamical core, with 66 vertical levels extending from the ground to 4.5×10^{-6} hPa (145 km geometric altitude), and a vertical resolution of 1.1–1.4 km in the tropical tropopause layer and the lower stratosphere (below a height of 30 km). The simulations presented in this paper are performed at a horizontal resolution of $1.9^\circ \times 2.5^\circ$ and with interactive chemistry (Garcia et al., 2007). More details regarding WACCM4 are provided in Marsh et al. (2013).

We calculate the statistical significance of the correlation between two auto-correlated time series using the two-tailed Student's t -test and the effective number (N^{eff}) of degrees of freedom (DOF; Bretherton et al. 1999). For this study, N^{eff} is determined using the following approximation (Li et al. 2012):

$$\frac{1}{N^{\text{eff}}} \approx \frac{1}{N} + \frac{2}{N} \sum_{j=1}^N \frac{N-j}{N} \rho_{xx}(j) \rho_{yy}(j)$$

where N is the sample size, and ρ_{XX} and ρ_{YY} are the autocorrelations of two sampled time series, X and Y , respectively, at time lag j .

We use the formulae given by Andrews et al. (1987) to calculate the quasi-geostrophic 2D Eliassen–Palm (E–P) flux. The meridional (F_y) and vertical (F_z) components of the E–P flux, and the E–P flux divergence D_F , are expressed as:

$$F_y = -\rho_0 a \cos \varphi \overline{\varphi u' v'}$$

$$F_z = -\rho_0 a \cos \varphi \frac{Rf}{HN^2} \overline{v' T'}$$

$$D_F = \frac{\nabla \cdot F}{\rho_0 a \cos \varphi} = \frac{\partial(F_y \cos \varphi) / a \cos \varphi \partial \varphi + \partial F_z / \partial z}{\rho_0 a \cos \varphi},$$

where ρ_0 is the air density, φ is the latitude, a is the radius of the Earth, R is the gas constant, f is the Coriolis parameter, H is the atmospheric scale height (7 km), u and v are the zonal and meridional wind components, respectively, and T is the temperature; the overbar denotes the zonal mean, and the prime symbol denotes departures from the zonal mean.

The Transformed Eulerian Mean (TEM) meridional wind (v^*) which is given by Edmon et al. (1980):

$$v^* = \bar{v} - [(\overline{v' \theta'}) / \bar{\theta}_p]_p$$

where θ is the potential temperature, v is meridional wind and subscript p denotes derivative with pressure p . The overbar denotes the zonal mean and the prime denotes deviations from the zonal mean value.

3. The connection between the East Asian Marginal Seas and southern high latitude lower stratospheric ozone in austral spring

Figure 2a shows the correlation coefficients between SST and southern high latitude

1 lower stratospheric ozone variations in austral spring between 1979 and 2015 using
2 ozone data from the MERRA2 dataset and SST from HadISST dataset. Ozone from
3 SLIMCAT simulations, GOZCARDS and SWOOSH datasets were further used to
4 confirm the robustness of the correlations (Fig. 2b–d). The regions of significant
5 correlation are generally different for the four ozone datasets except for the East Asian
6 Marginal Seas; i.e., 5°S–35°N, 100°E–140°E, where the most significant correlations
7 between Antarctic stratospheric ozone variations and SST are seen in the four datasets.
8 Fig. 2 implies an interannual connection between SST in the East Asian Marginal
9 Seas and southern high latitude lower stratospheric ozone variations in austral spring.
10 Fig. 2 also indicates that SST variations in austral spring associated with ENSO are
11 not the main factor controlling the interannual variability of southern high latitude
12 lower stratospheric ozone.

13 To investigate the SST variations across the marginal seas of East Asia, we first
14 define an austral spring SST index over the region with the most significant
15 correlations in Fig. 2, i.e., the ST_MSEA index (ST_MSEAI). This index is a time
16 series that represents SST variations across the marginal seas of East Asia in austral
17 spring (Figure 3a). It is calculated by averaging the SST variations in austral spring in
18 the region from 5°S–35°N at 100°E–140°E, and then removing the seasonal cycle and
19 linear trend. Fig. 3b and c show the composite warm and cold SST anomalies for the
20 events that occurred in the marginal seas of East Asia in austral spring between 1979
21 and 2015 (see Table 1).

22 It is well known that the SST changes in the eastern Pacific, the Indo-Pacific
23 warm pool, and the Atlantic can significantly influence the northern polar stratosphere
24 (Calvo et al., 2004, 2009; Hoerling et al., 2001, 2004; Cagnazzo et al., 2009; Hu and
25 Fu, 2009; Hu and Pan, 2009; Li et al., 2010; Hurwitz et al., 2011a, b; Lin et al., 2012;

1 Zubiaurre and Calvo, 2012; Xie et al., 2012; Li and Chen, 2014). SST variations in
2 some regions can excite Rossby wave trains and those waves can propagate into the
3 northern middle and high latitude stratosphere (Gettelman et al., 2001; Sassi et al.,
4 2004; Manzini et al., 2006; Garc ía-Herrera et al., 2006; Taguchi and Hartmann, 2006;
5 Garfinkel and Hartmann, 2007, 2008; Free and Seidel, 2009). The mechanism that
6 allows SST variations in the East Asian Marginal Seas to affect the southern high
7 latitude stratosphere is also possibly related to tropospheric wave propagation from
8 northern lower latitude to southern middle and high latitudes.

9 Figure 4 shows the ray paths of waves generated by the SST anomalies over the
10 region 5 °S–35 °N, 100 °E–140 °E, at 300 hPa in four seasons. The wavenumbers along
11 these rays are between 1 and 5. The wave ray paths represent the climate
12 teleconnections, i.e., the propagation of stationary waves in realistic flows. The
13 calculation of the wave ray paths and application of the barotropic model is described
14 in detail by Li et al. (2015) and Zhao et al. (2015). We found that the Rossby waves
15 generated by SST anomalies in the marginal seas of East Asia could indeed propagate
16 to the middle to high latitudes of the Southern Hemisphere in austral spring and
17 winter (Fig. 4a and d), but not in austral summer and autumn (Fig. 4b and c) because
18 the Rossby waves motivated by the low-latitude SST anomalies move mostly
19 northwards in austral summer and autumn. Meanwhile, we must note that the
20 propagating paths of those waves in austral spring and winter aren't totally same (Fig.
21 4a and d). In austral spring, the path of rays originates over the marginal seas of East
22 Asia reflects directly into the southern Indian Ocean and reaches the Southern
23 Hemisphere (Fig. 4a). In austral winter (Fig. 4d), the rays follow the austral spring
24 path to the Southern Hemisphere. In addition, the second path of rays originates over
25 the marginal seas of East Asia, crosses the Indian Ocean to arrive over tropical Africa

1 or even South America, and then reflects equatorward to the middle to high latitudes
2 of the Southern Hemisphere. We can see that these rays can reach about 60°S and then
3 be refracted to lower latitudes.

4 The correlation coefficients between the ST_MSEAI and 300-hPa geopotential
5 height variations associated with stationary waves of wavenumber 1 from the
6 ERA-Interim reanalysis across the four seasons are shown in Figure 5. The positive
7 and negative centers of correlation coefficients represent the teleconnection patterns.
8 The teleconnection patterns in austral spring and winter (Fig. 5a and d) are in good
9 agreement with the ray paths (Fig. 4a and d). In austral spring, a wave train path
10 appears over the marginal seas of East Asia and reflects directly into the Southern
11 Hemisphere (Fig. 5a). In austral winter, two clear wave train paths appear with one
12 moving westwards to South America and reflecting to the middle to high latitudes of
13 the Southern Hemisphere and the second reflecting to the middle to high latitudes of
14 the Southern Hemisphere. These two teleconnection pathways of the wave trains in
15 austral spring and winter (Figs. 4 and 5) are discussed in detail by Zhao et al., (2016),
16 who refer to them as the North Australia–Southern Hemisphere and South Africa–
17 Southern Hemisphere pathways, respectively. In austral summer and autumn, the
18 above two teleconnection patterns don't exist (Fig. 5b and c).

19 It is apparent that positive/negative correlation coefficients correspond to
20 positive/negative climatological wave 1 phases over Indo-Pacific warm pool but
21 negative/positive climatological wave 1 phases in the middle and high latitudes of
22 Southern Hemisphere in austral spring (Fig. 5a). The results in Fig. 5 implies that
23 warm/cold SST events over East Asian Marginal Seas would increase/decrease the
24 planetary wave activity at lower latitudes but decrease/increase the planetary wave
25 activity at middle and high latitudes of Southern Hemisphere.

Figs. 4 and 5 show the pathways of the wave trains generated by the SST anomalies over the marginal seas of East Asia in four seasons. Figure 6 shows the relationship between the SST anomalies and outgoing longwave radiation (OLR). The OLR can represent convective activity in the lower latitudes, while stronger convective activity often corresponds to enhanced wave activity. It is found that the correlation coefficients over the marginal seas of East Asia are the largest in the austral spring compared with other seasons. It implies that the wave activity anomalies caused by the SST anomalies over the marginal seas of East Asia are very strong in austral spring. Figs. 4, 5 and 6 illustrate the possibility of the SST anomalies over the marginal seas of East Asia influencing on the wave activity at southern high latitudes. Bodeker and Scourfield (1995), Shindell et al. (1997a, 1997b), and Huck et al. (2005) have shown that interannual differences in the severity of southern high latitude lower stratospheric ozone depletion are related to Southern Hemisphere planetary wave activity. All of the above analysis illustrates that the SST anomalies over the marginal seas of East Asia are a possible main source of this planetary wave activity.

Figure 7a shows the correlation coefficients between the ST_MSEAI and stratospheric ozone variations in austral spring, which indicate that warm (cold) SST anomalies over the East Asian Marginal Seas are associated with a decrease (increase) in southern high latitude lower stratospheric ozone in austral spring. Figure 7b shows that ST_MSEAI is positively correlated with zonal wind around 60°S, where is the climatological location of the boundary of the southern polar vortex in austral spring, while Figs. 7c indicate that ST_MSEAI is negatively correlated with the zonal mean temperature. The correlations shown in Figs 3, 4, 5, and 7 can be used to establish a hypothesis of chemical process for the connection between SST variations over the

1 marginal seas of East Asia and southern high latitude lower stratospheric ozone in
2 austral spring as follows: 1. The warm (cold) SST anomalies over the marginal seas of
3 East Asia (Fig. 3) depress (enhance) planetary wave activity in the middle to high
4 latitudes of the Southern Hemisphere (Figs. 4 and 5); 2. The anomalous propagation
5 of planetary waves into the stratosphere and dissipation of ultra-long Rossby waves in
6 the stratosphere strengthen/cool (weaken/warm) the southern polar vortex (Fig. 7b
7 and c); 3. A cooler (warmer) polar vortex allows more (less) PSCs and active chlorine
8 to form. 4. Consequently, southern high latitude lower stratospheric ozone decreases
9 (increases) (Fig. 7a).

10 However, it needs to point out that Antarctic polar vortex temperature is deeply
11 below the threshold for heterogeneous chemistry, so that a warming (cooling) in the
12 center of Antarctic polar vortex will have very little impact on Antarctic ozone by
13 affecting heterogeneous chemistry (Tilmes et al. 2006; Kirner et al. 2015). It seems to
14 challenge the above hypothesis. Fig. 7c shows that the center of the correlation
15 coefficients locates near 60 °S. It suggests that the center of stratospheric temperature
16 changes caused by SST changes in the East Asian Marginal Seas locates near 60 °S but
17 not near 90 °S. Temperature changes near 60 °S may have more effective effects on
18 southern high latitude lower stratospheric ozone than that near 90 °S since the
19 background temperature in the lower stratosphere near 60 °S would be higher than that
20 near 90 °S. The chemical process maybe has a contribution to the southern high
21 latitude lower stratospheric ozone changes caused by SST changes in the East Asian
22 Marginal Seas.

23 We also found that the SST changes in the East Asian Marginal Seas are
24 positively correlated with lower stratospheric TEM v^* between 30 °S and 60 °S (Fig.
25 7d), suggesting a stronger (weaker) zonal circulation (Fig. 7b) related to the SST

changes impeding (promoting) transport of ozone from the middle latitude stratosphere to high latitude stratosphere. Note that this correlation is the strongest in austral spring but not in austral winter when the south polar vortex is too stable to allow ozone rich air get into the vortex. Fig. 7d implies a dynamical contribution to the southern high latitude lower stratospheric ozone changes caused by SST changes in the East Asian Marginal Seas.

4. Simulating the effect of SST changes in the marginal seas of East Asia on southern high latitude lower stratospheric ozone

We performed three time-slice simulations with WACCM4 to further support the mechanism described in Section 3. The monthly mean climatologies of surface emissions used in the model were obtained from the A1B emissions scenario developed by the Intergovernmental Panel on Climate Change (IPCC), and averaged over the period 1979–2015. QBO signals with a 28-month fixed cycle are included in WACCM4 as an external forcing for zonal wind. The SST forcing used in the first time-slice experiment (S1, the control experiment) was the 12-month climatology cycle averaged over the period 1979–2015 and based on the HadISST dataset. S2 was a sensitivity experiment and was the same as S1 except that warm anomalies (as in Fig. 3b) were added to the SST in the marginal seas of East Asia (5°S–35°N and 100–140°E). The third experiment, S3, was the same as S2, but with cold SST anomalies (as in Fig. 3c). Detailed descriptions of experiments S1–S3 are provided in Table 2.

Figure 8 first shows the southern high latitude lower stratospheric ozone anomalies in austral spring forced by warm and cold SST anomalies over the marginal seas of East Asia. It can be seen that the warm SST anomalies indeed cause ozone decreases in the southern high latitude lower stratosphere (Fig. 8a) and cold SST

1 anomalies results in ozone increases (Fig. 8b). The simulations support the results
2 shown from the statistical analysis in Section 3.

3 Figure 9 shows the E–P flux vectors and divergence anomalies in the
4 stratosphere in austral spring caused by SST anomalies over the marginal seas of East
5 Asia. Analysis of changes in the E–P flux (Eliassen and Palm 1961; Andrews et al.
6 1987) is often used as a diagnostic for planetary wave propagation from the
7 troposphere to the stratosphere (Edmon et al., 1980). During periods of warm (cold)
8 SST over the marginal seas of East Asia, a decrease (increase) in upward wave flux
9 entering the stratosphere accompanied by stronger (weaker) divergence of the E–P
10 flux in the stratosphere at middle to high latitudes of the Southern Hemispheres (ca.
11 60°S) is evident (Fig. 9a and c). The anomalous wave flux entering the stratosphere
12 around 60°S confirms the result in Figs. 4 and 5, which shows that the wave rays can
13 reach about 60°S.

14 Many previous studies have demonstrated a strongly negative correlation
15 between upward propagating wave activity and the intensity of the stratospheric polar
16 vortex, with an anomalously negative and positive upward wave flux alongside a
17 stronger and weaker polar vortex, respectively (Christiansen 2001; Polvani and
18 Waugh 2004; Li and Lau 2013). During periods of warm (cold) SST over the marginal
19 seas of East Asia, the anomalous downward (upward) E–P flux, and larger (smaller)
20 E–P flux divergence at middle to high latitudes (ca. 60°S) in the Southern Hemisphere
21 (Fig. 9a and c) imply suppressed (active) wave activity in the stratosphere, which
22 induces a strengthened (weakened) circulation at southern polar vortex edge (Fig. 9b
23 and d). Finally, the cold (warm) polar vortex (Fig. 10a and c) allows more (less)
24 PSCs/active chlorine (Fig. 10b and d) to form. This is one process through which SST

1 variations over the marginal seas of East Asia causes southern high latitude lower
2 stratospheric ozone changes. The other process is that the strengthened (weakened)
3 southern polar vortex impedes (promotes) air exchange between middle and high
4 latitudes at 200 hPa to 50 hPa (Figure 11), and further decreases (increases) southern
5 high latitude lower stratospheric ozone levels.

6 It is noteworthy that warm (cold) SST anomalies are generally thought to
7 increase (suppress) planetary wave activity via strengthening (weakening) convection
8 (Xie et al., 2008; Shu et al., 2010; Hu et al., 2014). However, this study shows that
9 warm (cold) SST anomalies over the marginal seas of East Asia suppress (increase)
10 planetary wave activity in the southern high latitude stratosphere. Indeed, it is found
11 that there is an enhanced of the E-P flux from lower latitudes to southern high
12 latitudes in the SST warming event over the East Asian Marginal Seas (Figure 12a).
13 However, this increased EP flux does not propagate upward into the stratosphere but
14 downward to lower levels, and *vice versa* for the SST cooling event (Fig. 12b). Fig.
15 12 explains why SST warming (cooling) over the East Asian Marginal Seas leads to a
16 weaker (stronger) wave activity in the Southern Hemisphere stratosphere. This figure
17 is associated with the statistical analysis of Fig. 5a.

18 As a result of human activity, the amount of Antarctic stratospheric ozone has
19 decreased remarkably from 1950 to 2000 (Solomon 1990, 1999; Ravishankara et al.,
20 1994, 2009). At the same time, the SST over the marginal seas of East Asia has
21 followed an increasing trend, but superimposed on strong interannual variations
22 (Zheng et al., 2014). Figure 13 shows the correlation coefficients between southern
23 high latitude lower stratospheric ozone and SST in which the SST and southern high
24 latitude lower stratospheric ozone variations have not been detrended as that in Fig. 2.
25 Comparing Fig. 13 with Fig. 2, we can see that the negative correlation coefficients

over the marginal seas of East Asia become larger in Fig. 13, implying a contribution of warmer SST in the marginal seas of East Asia to the decline trend of southern high latitude lower stratospheric ozone.

We used ensemble transient experiments to estimate the contribution of SST variations in the marginal seas of East Asia to southern high latitude lower stratospheric ozone changes. The transient experiments incorporated the following natural and anthropogenic external forcings for the period 1955–2005: observed SST from the HadISST dataset, surface emissions from the IPCC A1B emissions scenario, spectrally resolved solar variability (Lean et al., 2005), volcanic aerosols (from the Stratospheric Processes and their Role in Climate (SPARC) Chemistry–Climate Model Validation (CCMVal) REF-B2 scenario recommendations), and nudged QBO (the time series in CESM is determined from the observed climatology). The first transient experiment, T1, was the historical experiment covering the period 1955–2005 (Marsh et al., 2013). The second transient experiment, T2, was the same as T1 except that the SST in the marginal seas of East Asia (5°S–35°N and 100–140°E) for the period 1955–2005 was replaced by the 12-month cycle of climatology averaged over the same period. This means that in T2, the SST over the marginal seas of East Asia had only a seasonal cycle, but no trend and no interannual variability. T3 was the same as T2, but used a slightly different initial condition as an ensemble experiment. Detailed descriptions of runs T1–T3 are provided in Table 3.

The southern high latitude lower stratospheric ozone variations caused by the SST variability over the marginal seas of East Asia can be obtained by subtracting simulated ozone in the ensemble experiments $((T2+T3)/2)$ from the ozone in T1 (Figure 14, black line). There are evident differences in southern high latitude lower stratospheric ozone variations between T1 and the ensemble experiments

1 ((T2+T3)/2)). This illustrates that the SST variability over the marginal seas of East
2 Asia (Fig. 14, red line) does have a significant effect on southern high latitude lower
3 stratospheric ozone over the past five decades (Fig. 14, black line). The correlation
4 coefficient between the two time series is 0.29 which is significant at 95% confidence
5 level. A further analysis reveals that the linear trend of ozone variations over the
6 region 200–50 hPa and 60–90 °S from T1 (Trend1) is -1.2×10^{-3} ppmv/month, from
7 T2 (Trend2) is -1.0×10^{-3} ppmv/month, from T3 (Trend3) is -0.89×10^{-3}
8 ppmv/month and from $(T1 - (T2+T3)/2)$ (Trend1_23, Fig. 14, black line) is $-0.2 \times$
9 10^{-3} ppmv/month. See Table 4. It implies that approximately 17% of the declining
10 trend in southern high latitude lower stratospheric ozone from 1955–2005 (Trend1_23
11 $\text{Trend1} \times 100\%$) may be related to the increasing linear trend in SST over the
12 marginal seas of East Asia.

13

14 **6. Conclusions and Summary**

15 In this study, the connection between SST and the southern high latitude lower
16 stratospheric ozone variations in austral spring on the interannual time scale is
17 examined. We found that SST over the marginal seas of East Asia can significantly
18 modulate the interannual variability of austral spring southern high latitude lower
19 stratospheric ozone and the processes involved in this modulation are related to
20 anomalous planetary wave activity induced by SST variations over the marginal seas
21 of East Asia. The planetary waves originating from the marginal seas can propagate
22 towards to the middle and high latitudes of the Southern Hemisphere in austral spring
23 via the North Australia–Southern Hemisphere and South Africa–Southern Hemisphere
24 pathways. The anomalous propagation and dissipation of ultra-long Rossby waves in
25 the stratosphere strengthens/cools (weakens/warms) the southern polar vortex, which

1 allows more (less) active chlorine to form and deplete more (less) ozone on one hand.
2 On the other hand, a stronger (weaker) polar vortex impedes (promotes) the transport
3 of middle latitude ozone to high latitudes and further decreases (increases) southern
4 high latitude lower stratospheric ozone. The above results are based on statistical
5 analysis but are also supported by time-slice experiments conducted using the CESM.

6 Our transient model simulations further demonstrated that SST variations over
7 the marginal seas of East Asia not only modulate the interannual variability of
8 southern high latitude lower stratospheric ozone, but also contribute to southern high
9 latitude lower stratospheric ozone trend over the past five decades. Our analysis
10 reveals that approximately 17% to the decreasing trend of southern high latitude lower
11 stratospheric ozone over the past five decades maybe associated with the trend of
12 increasing SST over the marginal seas of East Asia.

13

14 **Acknowledgments.** Funding for this project is provided by the Science Foundations
15 of China (41575038, 41375072, 41530423, and 41575039). The SLIMCAT modelling
16 work is supported by the UK National Centre for Atmospheric Science (NCAS) and
17 the CESM model is provide by NCAR. We acknowledge the datasets from the
18 ERA-interim, MERRA2, SWOOSH and GOZCARDS.

References

- Andrews, D. G., Holton, J. R., and Leovy, C. B.: Middle atmosphere dynamics, Academic press, 489 pp., 1987.
- Angell, J. K.: Relation of Antarctic 100 mb temperature and total ozone to equatorial QBO, equatorial SST, and sunspot number, 1958–87, *Geophys. Res. Lett.*, 15, 915–918, 1988.
- Angell, J. K.: Influence of equatorial QBO and SST on polar total ozone, and the 1990 Antarctic Ozone Hole, *Geophys. Res. Lett.*, 17, 1569–1572, 1990.
- Austin, J. and Wilson, R. J.: Ensemble simulations of the decline and recovery of stratospheric ozone, *J. Geophys. Res.*, 111, D16314, doi:10.1029/2005JD006907, 2006.
- Austin, J., Scinocca, J., Plummer, D., Oman, L., Waugh, D., Akiyoshi, H., Bekki, S., Braesicke, P., Butchart, N., Chipperfield, M., Cugnet, D., Dameris, M., Dhomse, S., Eyring, V., Frith, S., Garcia, R. R., Garny, H., Gettelman, A., Hardiman, S. C., Kinnison, D., Lamarque, J. F., Mancini, E., Marchand, M., Michou, M., Morgenstern, O., Nakamura, T., Pawson, S., Pitari, G., Pyle, J., Rozanov, E., Shepherd, T. G., Shibata, K., Teyss  re, H., Wilson, R. J., and Yamashita, Y.: Decline and recovery of total column ozone using a multimodel time series analysis, *J. Geophys. Res.*, 115, D00M10, doi:10.1029/2010JD013857, 2010.
- Bodeker, G. E. and Scourfield, M. W. J.: Planetary waves in total ozone and their relation to Antarctic ozone depletion, *Geophys. Res. Lett.*, 22, 2949–2952, 1995.
- Bowman, K. P.: Global patterns of the quasi-Biennial oscillation in total ozone, *J. Atmos. Sci.*, 46, 3328–3343, 1989.
- Bretherton, C. S., Widmann, M., Dymnikov, V. P., Wallace, J. M., and Blad   I.: The effective number of spatial degrees of freedom of a time-varying field, *J. Climate*, 12, 1990–2009, 1999.
- Cagnazzo, C., Manzini, E., Calvo, N., Douglass, A., Akiyoshi, H., Bekki, S., Chipperfield, M., Dameris, M., Deushi, M., Fischer, A. M., Garny, H., Gettelman, A., Giorgetta, M. A., Plummer, D., Rozanov, E., Shepherd, T. G., Shibata, K., Stenke, A., Struthers, H., and Tian, W.: Northern winter stratospheric temperature and ozone responses to ENSO inferred from an ensemble of chemistry climate models, *Atmos. Chem. Phys.*, 9, 8935–8948, 2009.

1 Cagnazzo, C., Manzini, E., Fogli, P. G., Vichi, and M., Davini, P.: Role of stratospheric dynamics
2 in the ozone-carbon connection in the Southern Hemisphere, *Clim. Dyn.*, 41, 3039–3054,
3 2013.

4 Calvo, N., Garcia, R., Garcia Herrera, R., Gallego, D., Gimeno, L., Hernández, E., and Ribera P.:
5 Analysis of the ENSO signal in tropospheric and stratospheric temperatures observed by
6 MSU, 1979– 2000, *J. Climate*, 17, 3934–3946, 2004.

7 Calvo, N., Giorgetta, M. A., Garcia-Herrera R., and Manzini, E.: Nonlinearity of the combined
8 warm ENSO and QBO effects on the Northern Hemisphere polar vortex in MAECHAM5
9 simulations, *J. Geophys. Res.*, 114, D13109, doi:10.1029/2008JD011445, 2009.

10 Chandra, S. and Mcpeters, R. D.: The solar-cycle variation of ozone in the stratosphere inferred
11 from Nimbus-7 and NOAA-11 satellites, *J. Geophys. Res.*, 99, 20665–20671, 1994.

12 Chipperfield, M.: New version of the TOMCAT/SLIMCAT off - line chemical transport model:
13 Intercomparison of stratospheric tracer experiments, *Q. J. Roy. Meteor. Soc.*, 132, 1179–1203,
14 2006.

15 Christiansen, B.: Downward propagation of zonal mean zonal wind anomalies from the
16 stratosphere to the troposphere: model and reanalysis, *J. Geophys. Res.*, 106, 27307–27322,
17 doi:10.1029/2000jd000214, 2001.

18 Clem K. R., Renwick J. A., and McGregor J.: Relationship between eastern tropical Pacific
19 cooling and recent trends in the Southern Hemisphere zonal-mean circulation, *Clim. Dyn.*, 1–
20 17, 2016.

21 Coy, L., Wargan, K., Molod, A., McCarty, W., and Pawson, S.: Structure and dynamics of the
22 Quasi-biennial Oscillation in MERRA-2, *J. Climate*, 29, 5339–5354, 2016.

23 Creilson, J. K., Fishman, J., and Wozniak, A. E.: Arctic Oscillation - induced variability in
24 satellite-derived tropospheric ozone, *Geophys. Res. Lett.*, 32, L14822,
25 doi:10.1029/2005GL023016, 2005.

26 Dee, D. P., et al.: The ERA-Interim reanalysis: Configuration and performance of the data
27 assimilation system, *Q. J. Roy. Meteor. Soc.*, 137, 553–597, 2011.

28 Dhomse, S. S., Weber, S. M., Wohltmann, I., Rex, M., and Burrows, J. P.: On the possible causes

1 of recent increases in northern hemispheric total ozone from a statistical analysis of satellite
2 data from 1979 to 2003, *Atmos. Chem. Phys.*, 6, 1165–1180, 2006.

3 Dhomse, S. S., Chipperfield, M. P., Feng, W., Hossaini, R., Mann, G. W., and Santee, M. L.:
4 Revisiting the hemispheric asymmetry in midlatitude ozone changes following the Mount
5 Pinatubo eruption: A 3–D model study, *Geophys. Res. Lett.*, 42, 3038–3047, 2015.

6 Dhomse, S. S., Chipperfield, M. P., Damadeo, R. P., Zawodny, J. M., Ball, W. T., Feng, W.,
7 Hossaini, R., Mann, G. W., and Haigh J. D.: On the ambiguous nature of the 11–year solar
8 cycle signal in upper stratospheric ozone, *Geophys. Res. Lett.*, 43, 7241–7249, 2016.

9 Douglass, A. R., Strahan, S. E., Oman, L. D., and Stolarski, R. S.: Understanding differences in
10 chemistry climate model projections of stratospheric ozone, *J. Geophys. Res.*, 119, 4922–
11 4939, 2014.

12 Edmon, H. J., Hoskins, B. J., and McIntyre, M. E.: Eliassen-Palm cross-sections for the
13 troposphere, *J. Atmos. Sci.*, 37, 2600–2616, 1980.

14 Eliassen, A. and Palm, E.: On the transfer of energy in stationary mountain waves, *Geofysiske*
15 *Publikasjoner*, 22, 1–23, 1961.

16 Evtushevsky, O. M., Kravchenko V. O., Hood L. L., Milinevsky G. P.: Teleconnection between the
17 central tropical Pacific and the Antarctic stratosphere: spatial patterns and time lags, *Clim.*
18 *Dyn.*, 44, 1841–1855, 2015.

19 Eyring, V., et al., : Multi-model assessment of stratospheric ozone return dates and ozone recovery
20 in CCMVal-2 models, *Atmos. Chem. Phys.*, 10, 9451–9472, 2010.

21 Farman, J. G., Gardiner, B. G., and Shanklin, J. D.: Large losses of total ozone in Antarctica reveal
22 seasonal ClO_x/NO_x interaction, *Nature*, 915, 207–210, 1985.

23 Feldstein, S. B.: Subtropical rainfall and the Antarctic ozone hole, *Science*, 332, 925–926, 2011.

24 Feng, W., Chipperfield, M. P., Davies, S., von der Gathen, P., Kyrö E., Volk, C. M., Ulanovsky, A.,
25 and Belyaev G.: Large chemical ozone loss in 2004/2005 Arctic winter/spring, *Geophys. Res.*
26 *Lett.*, 34, L09803, doi:10.1029/2006GL029098, 2007.

27 Feng, W., Chipperfield, M. P., Davies, S., Mann, G. W., Carslaw, K. S., Dhomse, S., Harvey, L.,
28 Randall, C., and Santee M. L.: Modelling the effect of denitrification on polar ozone

1 depletion for Arctic winter 2004/2005, *Atmos. Chem. Phys.*, 11, 6559–6573, 2011.

2 Forster, P. and Shine, K.: Radiative forcing and temperature trends from stratospheric ozone
3 changes, *J. Geophys. Res.*, 102, 10841–10855, 1997.

4 Free, M. and Seidel, D. J.: The observed ENSO temperature signal in the stratosphere, *J. Geophys.*
5 *Res.*, doi:10.1029/2009JD012420, 2009.

6 Frossard, L., Rieder, H. E., Ribatet, M., Staehelin, J., Maeder, J. A., Di Rocco, S., Davison, A. C.,
7 and Peter, T.: On the relationship between total ozone and atmospheric dynamics and
8 chemistry at mid-latitudes - Part 1: statistical models and spatial fingerprints of atmospheric
9 dynamics and chemistry, *Atmos. Chem. Phys.*, 13, 147–164, 2013.

10 Fujiwara, M., Kita, K., and Ogawa, T.: Stratosphere-troposphere exchange of ozone associated
11 with the equatorial Kelvin wave as observed with ozonesondes and rawinsondes, *J. Geophys.*
12 *Res.*, 103, 19173–19182, 1998.

13 Fusco, A. C. and Salby, M. L.: Interannual variations of total ozone and their relationship to
14 variations of planetary wave activity, *J. Climate*, 12, 1619 – 1629, 1999.

15 Garcia, R. R. and Solomon, S. A.: Possible relationship between interannual variability in
16 Antarctic ozone and the Quasi-biennial Oscillation, *Geophys. Res. Lett.*, 14, 848 –851, 1987.

17 Garcia, R. R., Marsh, D. R., Kinnison, D. E., Boville, B. A., and Sassi, F.: Simulation of secular
18 trends in the middle atmosphere, 1950–2003, *J. Geophys. Res.*, 112, D09301,
19 doi:10.1029/2006JD007485, 2007.

20 Garc á-Herrera, R., Calvo, N., Garcia, R. R., and Giorgetta, M. A.: Propagation of ENSO
21 temperature signals into the middle atmosphere: A comparison of two general circulation
22 models and ERA-40 reanalysis data, *J. Geophys. Res.*, 111, D06101,
23 doi:10.1029/2005JD006061, 2006.

24 Garfinkel, C. I. and Hartmann, D. L.: Effects of El Nino – Southern Oscillation and the
25 Quasi-biennial Oscillation on polar temperatures in the stratosphere, *J. Geophys. Res.*, 112,
26 D19112, doi:10.1029/2007JD008481, 2007.

27 Garfinkel, C. I. and Hartmann, D. L.: Different ENSO teleconnections and their effects on the
28 stratospheric polar vortex, *J. Geophys. Res.*, 113, D18114, doi:10.1029/2008JD009920,

1 2008.

2 Grassi, B., Redaelli G., and Visconti G.: Simulation of polar Antarctic trends: Influence of tropical

3 SST, *Geophys. Res. Lett.*, 32, L23806, doi:10.1029/2005GL023804, 2005.

4 Grassi, B., Redaelli G., and Visconti G.: A physical mechanism of the atmospheric response over

5 Antarctica to decadal trends in tropical SST, *Geophys. Res. Lett.*, 33, L17814,

6 doi:10.1029/2006GL026509, 2006.

7 Gettelman, A., Randel, W. J., Massie, S., and Wu, F.: El Niño as a natural experiment for studying

8 the tropical tropopause region, *J. Climate*, 14, 3375–3392, 2001.

9 Gray, L. J. and Ruth, S.: The modeled latitudinal distribution of the ozone Quasi-biennial

10 Oscillation using observed equatorial winds, *J. Atmos. Sci.*, 50, 1033–1046, 1993.

11 Hadjinicolaou, P., Pyle, J. A., Chipperfield, M. P., and Kettleborough, J. A.: Effect of interannual

12 meteorological variability on mid-latitude O₃, *Geophys. Res. Lett.*, 24, 2993–2996, 1997.

13 Hadjinicolaou, P., Jrrar, A., Pyle, J. A., and Bishop, L.: The dynamically driven long-term trend in

14 stratospheric ozone over northern middle latitudes, *Q. J. Roy. Meteor. Soc.*, 128, 1393–1412,

15 2002.

16 Hadjinicolaou, P., and Pyle, J. A.: The impact of Arctic ozone depletion on northern middle

17 latitudes: Interannual variability and dynamical control, *J. Atmos. Chem.*, 47, 25–43, 2004.

18 Hess, P. G. and Lamarque, J. F.: Ozone source attribution and its modulation by the Arctic

19 Oscillation during the spring months, *J. Geophys. Res.*, 112, D11303,

20 doi:10.1029/2006JD007557, 2007.

21 Hoerling, M. P., Hurrell, J. W., and Xu, T. Y.: Tropical origins for recent North Atlantic climate

22 change, *Science*, 292, 90–92, doi:10.1126/science.1058582, 2001.

23 Hoerling, M. P., Hurrell, J. W., Xu, T., Bates, G. T., and Phillips, A. S.: Twentieth century North

24 Atlantic climate change. Part II: Understanding the effect of Indian Ocean warming, *Clim.*

25 *Dynam.*, 23, 391–405, doi:10.1007/s00382-004-0433-x, 2004.

26 Hofmann, D. J. and Oltmans, S. J.: Anomalous Antarctic ozone during 1992 - Evidence for

27 Pinatubo volcanic aerosol effects, *J. Geophys. Res.*, 98, 18555–18561, 1993.

28 Hu, Y. and Fu, Q.: Stratospheric warming in Southern Hemisphere high latitudes since 1979,

1 Atmos. Chem. Phys., 9, 4329–4340, 2009.

2 Hu, Y., and Pan L.: Arctic stratospheric winter warming forced by observed SST, Geophys. Res.

3 Lett., 36, L11707, doi:10.1029/2009GL037832, 2009.

4 Hu, D., Tian, W., Xie, F., Shu, J., and Dhomse, S.: Effects of meridional sea surface temperature

5 changes on the stratospheric temperature and circulation, Adv. Atmos. Sci., 31, 888–900,

6 doi:10.1007/s00376-013-3152-6, 2014.

7 Huck, P. E., McDonald, A. J., Bodeker, G. E., and Struthers, H.: Interannual variability in

8 Antarctic ozone depletion controlled by planetary waves and polar temperature, Geophys.

9 Res. Lett., 32, 370–370, 2005.

10 Hurwitz, M. M., Newman, P. A., Oman, L. D., and Molod, A. M.: Response of the Antarctic

11 stratosphere to two types of El Niño events, J. Atmos. Sci., 68, 812–822,

12 doi:10.1175/2011JAS3606.1, 2011a.

13 Hurwitz, M. M., Song, I. S., Oman, L. D., Newman, P. A., Molod, A. M., Frith, S. M., and Nielsen,

14 J. E.: Response of the Antarctic stratosphere to warm pool El Niño Events in the GEOS CCM,

15 Atmos. Chem. Phys., 11, 9659–9669, doi:10.5194/acp-11-9659-2011, 2011b.

16 Kang, S. M., Polvani, L. M., Fyfe, J. C., and Sigmond, M.: Impact of polar ozone depletion on

17 subtropical precipitation, Science, 332, 951–954, 2011.

18 Keeble, J., Braesicke, P., Abraham, N. L., Roscoe, H. K., and Pyle, J. A.: The impact of polar

19 stratospheric ozone loss on Southern Hemisphere stratospheric circulation and climate,

20 Atmos. Chem. Phys., 14, 13705–13717, 2014.

21 Kerr, B. and McElroy, C. T.: Evidence for large upward trends of ultraviolet-B radiation linked to

22 ozone depletion, Science, 262, 1032–1034, 1993.

23 Kirner, O., Müller, R., Ruhnke, R., and Fischer, H.: Contribution of liquid, NAT and ice particles

24 to chlorine activation and ozone depletion in Antarctic winter and spring, Atmos. Chem.

25 Phys., 15, 2019–2030, 2015.

26 Lait, L. R., Schoeberl, M. R., and Newman, P. A.: Quasi-biennial modulation of the Antarctic

27 ozone depletion, J. Geophys. Res., 94, 11559–11571, 1989.

28 Lamarque, J. F. and Hess, P. G.: Arctic Oscillation modulation of the Northern Hemisphere spring

1 tropospheric ozone, *Geophys. Res. Lett.*, 31, L06127, doi:10.1029/2003GL019116, 2004.

2 Lean, J., Rottman, G., Harder, J., and Kopp, G.: *SORCE contributions to new understanding of*
3 *global change and solar variability*, *Sol. Phys.*, 230, 27–53, 2005.

4 Li, F., Vikhliaev, Y. V., Newman, P. A., Pawson, S., Perlwitz, J., Waugh, D. W., and Douglass, A.
5 R.: *Impacts of interactive stratospheric chemistry on Antarctic and southern ocean climate*
6 *change in the Goddard Earth Observing System, Version 5 (GEOS-5)*, *J. Climate*, 29, 3199–
7 3218, 2016.

8 Li, K. F. and Tung, K. K.: *Quasi-biennial Oscillation and solar cycle influences on winter Arctic*
9 *total ozone*, *J. Geophys. Res.*, 119, 5823–5835, 2014.

10 Li, K. F., Tian, B., Waliser, D. E., Schwartz, M. J., Neu, J. L., Worden, J. R., and Yung, Y. L.:
11 *Vertical structure of MJO-related subtropical ozone variations from MLS, TES, and*
12 *SHADOZ data*, *Atmos. Chem. Phys.*, 12, 425–436, 2012.

13 Li, Y. J., Li, J., Jin, F. F., and Zhao, S.: *Interhemispheric propagation of stationary rossby waves in*
14 *a horizontally no uniform background flow*, *J. Atmos. Sci.*, 72, 3233–3256, 2015.

15 Li, Y. and Lau, N. C.: *Influences of ENSO on stratospheric variability, and the descent of*
16 *stratospheric perturbations into the lower troposphere*, *J. Climate*, 26, 4725–4748, 2013.

17 Li, S. L., Perlwitz, J., Hoerling, M. P., and Chen, X. T.: *Opposite annular responses of the*
18 *Northern and Southern Hemispheres to Indian Ocean warming*, *J. Climate*, 23, 3720–3738,
19 2010.

20 Li, S. L. and Chen, X. T.: *Quantifying the response strength of the southern stratospheric polar*
21 *vortex to Indian Ocean warming in austral summer*, *Adv. Atmos. Sci.*, 31, 492–503, 2014.

22 Lin, P., Fu, Q., and Hartmann, D.: *Impact of tropical SST on stratospheric planetary waves in the*
23 *Southern Hemisphere*, *J. Climate*, 25, 5030–5046, doi:http://dx.doi.org/10.1175/JCLI-D-11-0
24 0378.1, 2012.

25 Li, Y., Li, J., and Feng, J. A.: *Teleconnection between the reduction of rainfall in Southwest*
26 *Western Australia and North China*, *J. Climate*, 25, 8444–8461, 2012.

27 Liu, C. X., Liu, Y., Cai, Z. N., Gao, S. T., Lu, D. R., and Kyrola, E.: *A Madden-Julian*
28 *Oscillation-triggered record ozone minimum over the Tibetan Plateau in December 2003 and*

1 its association with stratospheric "low-ozone pockets", *Geophys. Res. Lett.*, 36, L15830,
2 doi:10.1029/2009GL039025, 2009.

3 Liu, J. J., Jones, D. B. A., Zhang, S., and Kar, J.: Influence of interannual variations in transport on
4 summertime abundances of ozone over the Middle East, *J. Geophys. Res.*, 116, D20310,
5 doi:10.1029/2011JD016188, 2011.

6 Liu, J., Tarasick, D. W., Fioletov, V. E., McLinden, C., Zhao, T., Gong, S., Sioris, C., Jin, J. J., Liu,
7 G., and Moeini O.: A global ozone climatology from ozone soundings via trajectory mapping:
8 a stratospheric perspective, *Atmos. Chem. Phys.*, 13, 11441–11464, 2013.

9 Mancini, E., Visconti, G., Pitart, G., and Verdecch, M.: An estimate of the Antarctic ozone
10 modulation by the QBO, *Geophys. Res. Lett.*, 18, 175–178, 1991.

11 Manzini, E., Giorgetta, M. A., Esch, M., Kornblueh, L., and Roeckner, E.: The influence of sea
12 surface temperatures on the northern winter stratosphere: Ensemble simulations with the
13 MAECHAM5 model, *J. Climate*, 19, 3863–3881, 2006.

14 Manney, G., Zurek, R., O'Neill, A., and Swinbank, R.: On the motion of air through the
15 stratospheric polar vortex. *J. Atmos. Sci.*, 51, 2973–2994, 1994.

16 Marsh, D. R., Mills, M. J., Kinnison, D. E., Lamarque, J.-F., Calvo, N., and Polvani, L. M.:
17 Climate change from 1850 to 2005 simulated in CESM1 (WACCM), *J. Climate*, 26, 7372–73
18 91, 2013.

19 Müller, R., Peter, T., Crutzen, P. J., Oelhaf, H., Adrian, G. P., Von Clarmann, T., Wegner, A.,
20 Schmidt, U., and Lary, D.: Chlorine chemistry and the potential for ozone depletion in the
21 arctic stratosphere in the winter of 1991/92, *Geophys. Res. Lett.*, 21, 1427–1430, 1994.

22 Müller, R., Tilmes, S., Konopka, P., Grooß J.-U., and Jost H.-J.: Impact of mixing and chemical
23 change on ozone-tracer relations in the polar vortex, *Atmos. Chem. Phys.*, 5, 3139–3151,
24 2005.

25 Perlwitz, J., Pawson, S., Fogt, R. L., Nielsen, J. E., and Neff, W. D.: Impact of stratospheric ozone
26 hole recovery on Antarctic climate, *Geophys. Res. Lett.*, 35, L08714,
27 doi:10.1029/2008GL033317, 2008.

28 Polvani, L. M. and Waugh, D. W.: Upward wave activity flux as a precursor to extreme

1 stratospheric events and subsequent anomalous surface weather regimes, *J. Climate*, 17,
2 3548–3554, 2004.

3 Polvani, L. M., Waugh, D. W., Correa, G. J. P., and Son, S.-W.: Stratospheric ozone depletion: The
4 main driver of twentieth-century atmospheric circulation changes in the Southern
5 Hemisphere, *J. Climate*, 24, 795–812, doi:10.1175/2010JCLI3772.1, 2011.

6 Prather, M. J.: Numerical advection by conservation of second-order moments, *J. Geophys. Res.*,
7 91, 6671–6681, 1986.

8 Previdi, M. and Polvani, L. M.: Climate system response to stratospheric ozone depletion and
9 recovery, *Q. J. Roy. Meteor. Soc.*, 140, 2401–2419, doi:10.1002/qj.2330, 2014.

10 Randel, W. J., Garcia, R. R., Calvo, N., and Marsh, D.: ENSO influence on zonal mean
11 temperature and ozone in the tropical lower stratosphere, *Geophys. Res. Lett.*, 36, L15822,
12 doi:10.1029/2009GL039343, 2009.

13 Rao, J., and Ren R., A decomposition of ENSO’s impacts on the northern winter stratosphere:
14 competing effect of SST forcing in the tropical Indian Ocean, *Clim. Dyn.*, 1–19,
15 doi:10.1007/s00382-015-2797-5, 2015.

16 Rayner, N. A., Parker, D. E., Horton, E. B., Folland, C. K., Alexander, L. V., Rowell, D. P., Kent,
17 E. C., and Kaplan, A.: Global analysis of sea surface temperature, sea ice, and night marine
18 air temperature since the late nineteenth century, *J. Geophys. Res.*, 108,
19 doi:10.1029/2002JD002670, 2003.

20 Ren, R. C., Cai M., Xiang C. Y., and Wu G. X.: Observational evidence of the delayed response of
21 stratospheric polar vortex variability to ENSO SST anomalies, *Clim. Dyn.*, 38, 1345–1358,
22 doi:10.1007/s00382-011-1137-7, 2012.

23 Rieder, H. E., Frossard, L., Ribatet, M., Staehelin, J., Maeder, J. A., Di Rocco, S., Davison, A. C.,
24 Peter, T., Weihs, P., and Holawe F.: On the relationship between total ozone and atmospheric
25 dynamics and chemistry at mid-latitudes - Part 2: The effects of the El Nino/Southern
26 Oscillation, volcanic eruptions and contributions of atmospheric dynamics and chemistry to
27 long-term total ozone changes, *Atmos. Chem. Phys.*, 13, 165–179, 2013.

28 Rienecker, M. M., et al.: MERRA: NASA's modern-era retrospective analysis for research and

1 applications, *J. Climate*, 24, 3624–3648, 2011.

2 Rozanov, E. V., Schlesinger, M. E., Andronova, N. G., Yang, F., Malyshev, S. L., Zubov, V. A.,
3 Egorova, T. A., and Li, B.: Climate/chemistry effects of the Pinatubo volcanic eruption
4 simulated by the UIUC stratosphere/troposphere GCM with interactive photochemistry, *J.*
5 *Geophys. Res.*, 107, 4594, doi:10.1029/2001JD000974, 2002.

6 Rozanov, E. V., Schraner, M., Egorova, T., Ohmura, A., Wild, M., Schmutz, W., and Peter, T.:
7 Solar signal in atmospheric ozone, temperature and dynamics simulated with CCM SOCOL
8 in transient mode, *Memor. Soc. Astronom. Ital.*, 76, 876–879, 2005.

9 Salby, M. L. and Callaghan, P. F.: Systematic changes of Northern Hemisphere ozone and their
10 relationship to random interannual changes, *J. Climate*, 17, 4512–4521, 2004.

11 Salby, M. L. and Callaghan, P. F.: Influence of planetary wave activity on the stratospheric final
12 warming and spring ozone, *J. Geophys. Res.*, 112, 365-371, 2007a.

13 Salby, M. L. and Callaghan, P. F.: On the wintertime increase of Arctic ozone: Relationship to
14 changes of the polar-night vortex, *J. Geophys. Res.*, 112, 541-553, 2007b.

15 Sassi, F., Kinnison, D., Boville, B. A., Garcia, R. R., and Roble, R.: Effect of El Niño-Southern
16 Oscillation on the dynamical, thermal, and chemical structure of the middle atmosphere, *J.*
17 *Geophys. Res.*, 109, D17108, doi:10.1029/ 2003JD004434, 2004.

18 Schnadt, C., and Dameris M.: Relationship between North Atlantic Oscillation changes and
19 stratospheric ozone recovery in the Northern Hemisphere in a chemistry-climate model,
20 *Geophys. Res. Lett.*, 30, 1487, doi:10.1029/ 2003GL017006, 2003.

21 Schoeberl, M. R. and Hartmann, D. L.: The dynamics of the stratospheric polar vortex and its
22 relation to springtime ozone depletions, *Science*, 251, 46–52, 1991.

23 Shindell, D. T. and Schmidt, G. A.: Southern Hemisphere climate response to ozone changes and
24 greenhouse gas increases, *Geophys. Res. Lett.*, 31, L18209, doi:10.1029/2004GL020724,
25 2004.

26 Shindell, D. T., Wong, S., and Rind, D.: Interannual variability of the Antarctic ozone hole in a
27 GCM. Part I: The influence of tropospheric wave variability, *J. Atmos. Sci.*, 54, 2308–2319,
28 1997.

1 Shindell, D. T., Rind, D., and Balachandran, N.: Interannual variability of the Antarctic ozone hole
2 in a GCM. Part II: A comparison of unforced and QBO-Induced variability, *J. Atmos. Sci.*, 56,
3 1873–1884, 2010.

4 Shu, J., Tian, W., Hu, D., Zhang, J., Shang, L., Tian, H., and Xie, F.: Effects of the Quasi-biennial
5 Oscillation and stratospheric semiannual oscillation on tracer transport in the upper
6 stratosphere, *J. Atmos. Sci.*, 70, 1370–1389, doi:10.1175/JAS-D-12-053.1, 2013.

7 Sigmond, M. and Fyfe, J. C.: The Antarctic sea ice response to the ozone hole in climate models, *J.*
8 *Climate*, 27, 1336–1342, 2014.

9 Solomon, S.: Antarctic ozone: progress towards a quantitative understanding, *Nature*, 347, 347–
10 354, 1990.

11 Solomon, S.: Stratospheric ozone depletion: A review of concepts and history, *Rev. Geophys.*, 37,
12 275–316, 1999.

13 Son, S.-W., Polvani, L. M., Waugh, D. W., Akiyoshi, H., Garcia, R., Kinnison, D., Pawson, S.,
14 Rozanov, E., Shepherd, T. G., and Shibata, K.: The impact of stratospheric ozone recovery on
15 the Southern Hemisphere westerly jet, *Science*, 320, 1486–1489, 2008.

16 Son, S.-W., Tandon, N. F., Polvani, L. M., and Waugh, D. W.: Ozone hole and Southern
17 Hemisphere climate change, *Geophys. Res. Lett.*, 36, L15705, doi:10.1029/2009GL038671,
18 2009.

19 Son, S.-W., et al.: Impact of stratospheric ozone on Southern Hemisphere circulation change: A
20 multimodel assessment, *J. Geophys. Res.*, 115, D00M07, doi:10.1029/2010JD014271, 2010.

21 Steinbrecht, W., Kohler U., Claude H., Weber M., Burrows J. P., and van der A, R. J.: Very high
22 ozone columns at northern mid-latitudes in 2010, *Geophys. Res. Lett.*, 38, L06803,
23 doi:10.1029/2010GL046634, 2011.

24 Thompson, D. W. J., Solomon, S., Kushner, P. J., England, M. H., Grise, K. M., and Karoly, D. J.:
25 Signatures of the Antarctic ozone hole in Southern Hemisphere surface climate change,
26 *Nature Geosci.*, 4, 741–749, 2011.

27 Tian, W. and Chipperfield, M. P.: A new coupled chemistry–climate model for the stratosphere:
28 The importance of coupling for future O3-climate predictions, *Q. J. Roy. Meteor. Soc.*, 131,

1 281–303, 2005.

2 Tian, B. J., Yung, Y. L., Waliser, D. E., Tyranowski, T., Kuai, L., Fetzer, E. J., and Irion, F. W.:
3 Intraseasonal variations of the tropical total ozone and their connection to the Madden-Julian
4 Oscillation, *Geophys. Res. Lett.*, 34, L08704, doi:10.1029/2007GL029451, 2007.

5 Tilmes, S., Müller, R., Engel, A., Rex, M., and Russell III J. M.: Chemical ozone loss in the Arctic
6 and Antarctic stratosphere between 1992 and 2005, *Geophys. Res. Lett.*, 33, L20812, 2006.

7 Trenberth, K. E: The definition of El Niño, *Bull. Am. Meteorol. Soc.*, 78, 2771–2777, 1997.

8 Tung, K. K. and Yang, H.: Dynamic variability of column ozone, *J. Geophys. Res.*, 93, 11123–
9 11128, 1988.

10 Wargan, K., Labow, G., Frith, S., Pawson, S., Livesey, N., and Partyka, G.: Evaluation of the
11 ozone fields in NASA’s MERRA-2 reanalysis, *J. Climate.*, DOI:
12 <http://dx.doi.org/10.1175/JCLI-D-16-0699.1>, 2017.

13 Weare, B. C.: Madden-Julian Oscillation in the tropical stratosphere, *J. Geophys. Res.*, 115,
14 D17113, doi:10.1029/2009JD013748, 2010.

15 Weber, M., Dhomse, S., Wittrock, F., Richter, A., Sinnhuber, B.-M., and Burrows, J. P.:
16 Dynamical control of NH and SH Winter/Spring total ozone from GOME observations in
17 1995 – 2002, *Geophys. Res. Lett.*, 30, 389–401, 2003.

18 Weiss, A. K., Staehelin, J., Appenzeller, C., and Harris, N. R. P.: Chemical and dynamical
19 contributions to ozone profile trends of the Payerne (Switzerland) balloon soundings, *J.*
20 *Geophys. Res.*, 106, 22685–22694, 2001.

21 Welhouse, L. J., Lazzara M. A., Keller L. M., Tripoli G. J., Hitchman M. H.: Composite analysis
22 of the effects of ENSO events on Antarctica, *J. Climate*, 29, 1797–1808, 2016.

23 Wilson, A. B., Bromwich D. H., Hines K. M., Wang S.: El Niño flavors and their simulated
24 impacts on atmospheric circulation in the high southern latitudes, *J. Climate*, 27, 8934–8955,
25 2014.

26 Yang, C, Li T, Dou X, Xue X.: Signal of central Pacific El Niño in the Southern Hemispheric
27 stratosphere during austral spring, *J. Geophys. Res.*, 120, 2015.

28 Yu, J. Y., Paek H., Saltzman E. S., Lee T.: The early 1990s change in ENSO–PSA–SAM

relationships and its impact on Southern Hemisphere climate, *J. Climate*, 28, 9393–9408, 2015.

Xie, F., Tian, W., and Chipperfield, M. P.: Radiative effect of ozone change on stratosphere-troposphere exchange, *J. Geophys. Res.*, 113, D00B09, doi:10.1029/2008JD009829, 2008.

Xie, F., Li, J., Tian, W., Feng, J., and Huo, Y.: The signals of El Niño Modoki in the tropical tropopause layer and stratosphere, *Atmos. Chem. Phys.*, 12, 5259–5273, doi:10.5194/acp-12-5259-2012, 2012.

Xie, F., Li, J., Tian, W., Zhang, J., and Shu, J.: The impacts of two types of El Nino on global ozone variations in the last three decades, *Adv. Atmos. Sci.*, 31, 1113–1126, 2014a.

Xie, F., Li, J., Tian, W., Zhang, J., and Sun, C.: The relative impacts of El Nino Modoki, canonical El Nino, and QBO on tropical ozone changes since the 1980s, *Environ. Res. Lett.*, 9, 064020, 2014b.

Xie F., Li, J., Tian, W., Fu, Q., Jin, F-F., Hu, Y., Zhang, J., Wang, W., Sun, C., Feng, J., Yang Y., and Ding, R.: A connection from Arctic stratospheric ozone to El Niño-Southern Oscillation, *Environ. Res. Lett.*, 11, 124026, 2016.

Zhao, S., Li, J., and Li, Y. J.: Dynamics of an interhemispheric teleconnection across the critical latitude through a southerly duct during boreal winter. *J. Climate*, 28, 7437–7456, 2015.

Zhao, S., Li, J., Li, Y., and Zheng, J.: Interhemispheric influence of the Indo-Pacific convection oscillation on Southern Hemisphere rainfall, Submitted to *Climate Dynamics*, 2016.

Zheng, J. Y., Li, J., and Feng, J.: A dipole pattern in the Indian and Pacific oceans and its relationship with the East Asian summer monsoon, *Environ. Res. Lett.*, 9, 074006, doi:10.1088/1748-9326/9/7/074006, 2014.

Zhang, J., Tian, W., Xie, F., Tian, H., Luo, J., Zhang, J., Liu, W., and Dhomse, S.: Climate warming and decreasing total column ozone over the Tibetan Plateau during winter and spring, *Tellus*, 66B, 136–140, 2014.

Zhang, J., Tian, W. S., Wang, Z. W., Xie, F., and Wang, F. Y.: The influence of ENSO on Northern midlatitude ozone during the winter to Spring transition, *J. Climate*, 28, 4774–4793, 2015a.

- 1 Zhang, J., Tian, W. S., Xie, F., Li, Y. P., Wang, F. Y., Huang, J. L., and Tian, H. Y.: 2015b:
2 Influence of the El Niño–Southern Oscillation on the total ozone column and clear-sky
3 ultraviolet radiation over China, *Atmos. Environ.*, 120, 205–216, 2015b.
- 4 Zubiaurre, I. and Calvo, N.: The El Niño–Southern Oscillation (ENSO) Modoki signal in the
5 stratosphere, *J. Geophys. Res.*, 117, D04104, doi:10.1029/2011JD016690, 2012.

1 Table 1. Warm and cold SST events in the marginal seas of East Asia in austral spring during the
2 period from 1979 to 2015 analyzed in this paper using the ST_MSEAI (Fig. 3a).

Warm Events [*]	Cold Events [*]
1983	1982
1987	1991
1988	1992
1998	1994
1999	2004
2008	2012

3 ^{*}Following the definition of ENSO events (Trenberth 1997), we propose a threshold of ± 0.2 ,
4 which is equal to the standard deviation of the ST_MSEAI series, as the indicator of warm and
5 cold events.

1 **Table 2.** Experiments S1–S3.

Experiments ^{*1}	Descriptions
S1	Time-slice run using case F_2000_WACCM in CESM. The SST is the 12-month cycle climatology mean for the period 1979–2015 based on HadISST dataset (Rayner et al., 2003); the monthly mean climatologies of surface emissions used in the model are obtained from the A1B emissions scenario developed by the IPCC, averaged over the period 1979–2015. QBO phase signals with a 28-month fixed cycle are included in WACCM4 as an external forcing for zonal wind.
S2	Same as S1, except that the SST in the marginal seas of East Asia (5 °S–35 °N and 100–140 °E) adds warm SST anomalies (as Fig. 3b).
S3	Same as S1, except that the SST in the marginal seas of East Asia (5 °S–35 °N and 100–140 °E) adds cold SST anomalies (as Fig. 3c).

2 ^{*1}Each experiment is run for 53 years, with the first 3 years excluded as a spin-up period. The
3 remaining 50 years are used for the analysis.

1 **Table 3.** Experiments T1–T3.

Experiments ^{*1}	Descriptions
T1	Transient run using case F_1955-2005_WACCM_CN in CESM. SST forcing based on HadISST dataset, surface emissions are obtained from the A1B emissions scenario developed by the IPCC, spectrally resolved solar variability (Lean et al., 2005), volcanic aerosols (from the SPARC CCMVal REF-B2 scenario recommendations), nudged QBO (the time series in CESM is determined from the observed climatology).
T2	Same as T1, except that the SST in the marginal seas of East Asia (5°S–35°N and 100–140°E) between 1955 and 2005 is replaced by the 12 months cycle of climatology averaged for the period 1955–2005.
T3	Same as T2, but with slightly different initial condition ^{*2}

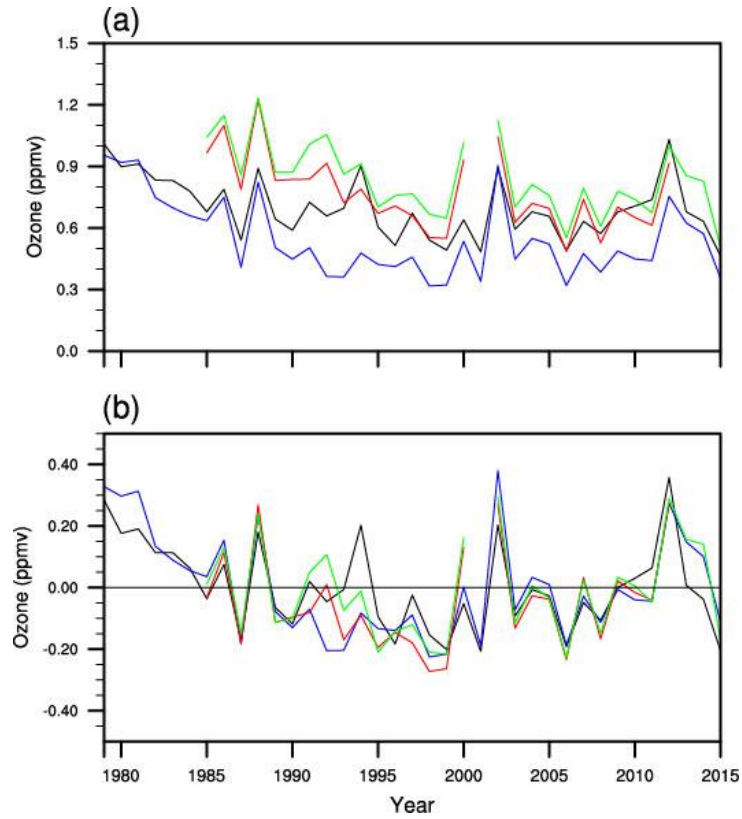
2 ^{*1}Integration period is 1955–2005 for T1–T3.

3 ^{*2}The parameter <pertlim> is used to produce different initial conditions in the CESM model,
4 which produces an initial temperature perturbation. The magnitude was about e^{-14} .

1 Table 4. Linear trends of ozone variations over the region 200–50 hPa and 60–90 °S from
 2 experiments with (T1) and without SST (T2 +T3) variations in the East Asian Marginal Seas (T1–
 3 3 see Table 3).

Experiments	Values
Linear trend of ozone variations over the region 200–50 hPa and 60–90 °S from T1 (Trend1)	-1.2×10^{-3} ppmv/month ^{**}
Same as Trend1, but from T2 (Trend 2)	-1.0×10^{-3} ppmv/month [*]
Same as Trend1, but from T3 (Trend 3)	-0.89×10^{-3} ppmv/month [*]
Same as Trend1, but from (T1 – (T2+T3)/2) (Trend1_23)	-0.2×10^{-3} ppmv/month [*]

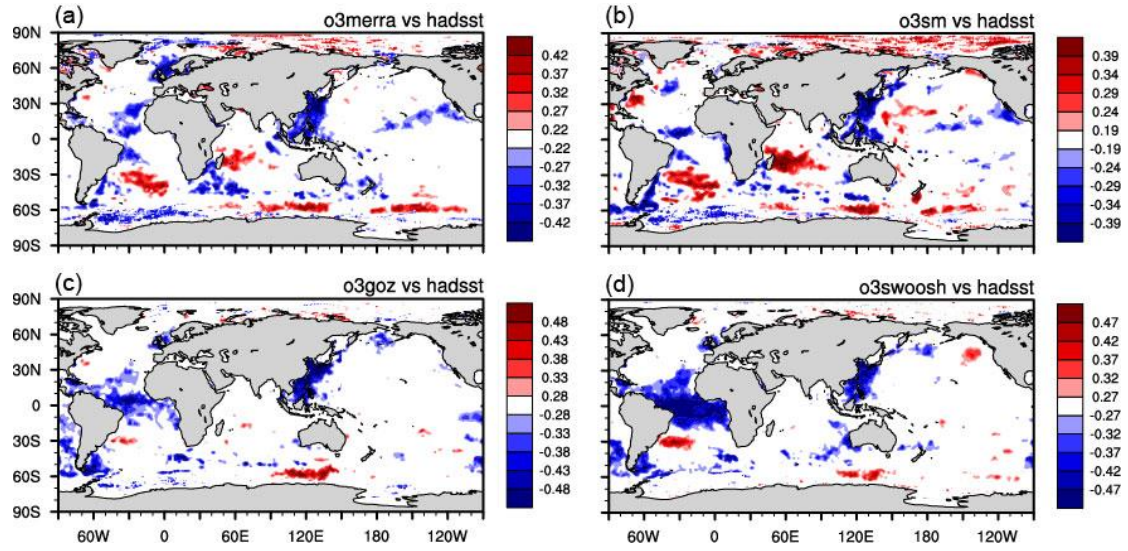
4 ^{**}: the trend is significant at 99% confidence level. ^{*}: the trend is significant at 95% confidence
 5 level. The calculation of the statistical significance of the trend uses the two-tailed Student's *t*-test.



1

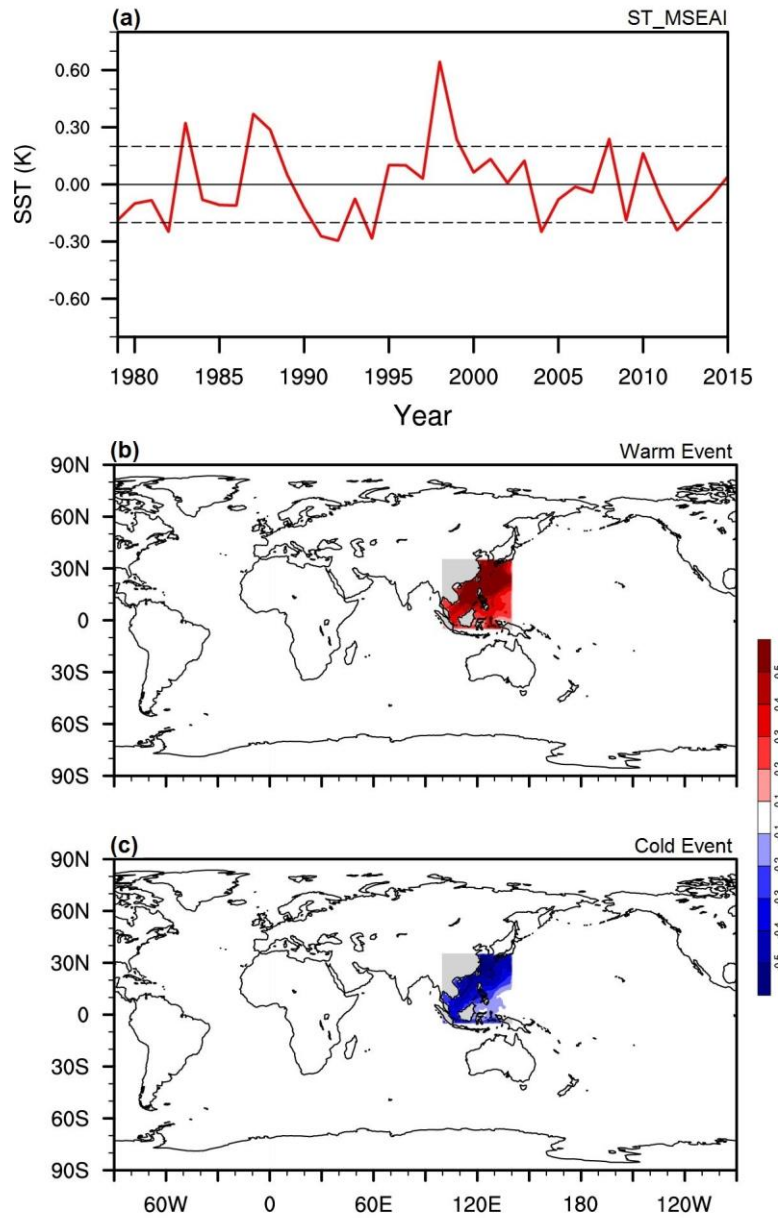
2 **Figure 1.** (a) Time series of original ozone concentrations at southern high latitude lower
3 stratosphere in austral spring averaged over the region 60–90 °S at 200–50 hPa for the MERRA2
4 (black line) and SLIMCAT (blue line) ozone datasets and over the region 60–75 °S at 200–50 hPa
5 for GOZCARDS (red line) and SWOOSH (green line) ozone datasets. (b), Same as (a), but the
6 ozone variations are removed the seasonal cycles and linear trends.

1



2

3 **Figure 2.** Correlation coefficients between southern high latitude lower stratospheric ozone and
4 SST variations in austral spring. Southern high latitude lower stratospheric ozone variations in
5 austral spring are averaged over the region 60–90 °S at 200–50 hPa for the MERRA2 (a) and
6 SLIMCAT (b) ozone datasets and over the region 60–75 °S at 200–50 hPa for GOZCARDS (c) and
7 SWOOSH (d) ozone datasets. SST from HadISST. Only statistical significance above 95%
8 confidence level is colored; statistical significance was calculated using the two-tailed Student's
9 t -test and the N^{eff} of DOF. The seasonal cycles and linear trends were removed prior to calculating
10 the correlation coefficients.



1

2 **Figure 3.** (a) SST variations in the marginal seas of East Asia in austral spring defined using the
3 ST_MSEA index (ST_MSEAI) that was calculated by averaging SST over the region from 5°S–
4 35°N at 100°E–140°E (from HadISST), and then removing seasonal cycles and linear trend. The
5 dashed lines indicate the thresholds for definition of warm and cold events. (b) and (c) show the
6 composite warm and cold SST anomalies in austral spring, respectively, for the events listed in
7 Table 1.

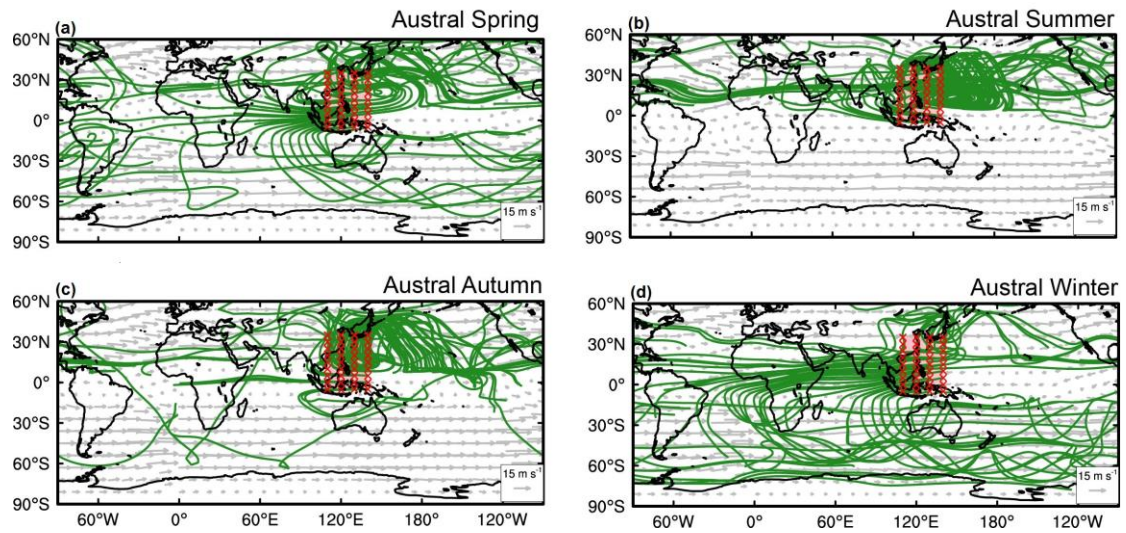


Figure 4. Ray paths (green lines) at 300 hPa in (a) austral spring, (b) austral summer, (c) austral autumn, and (d) austral winter. Red points denote wave sources in the marginal seas of East Asia (5°S–35°N, 100°E–140°E). The wavenumbers along these rays are in the range 1–5. The grey vectors indicate climatological flows.

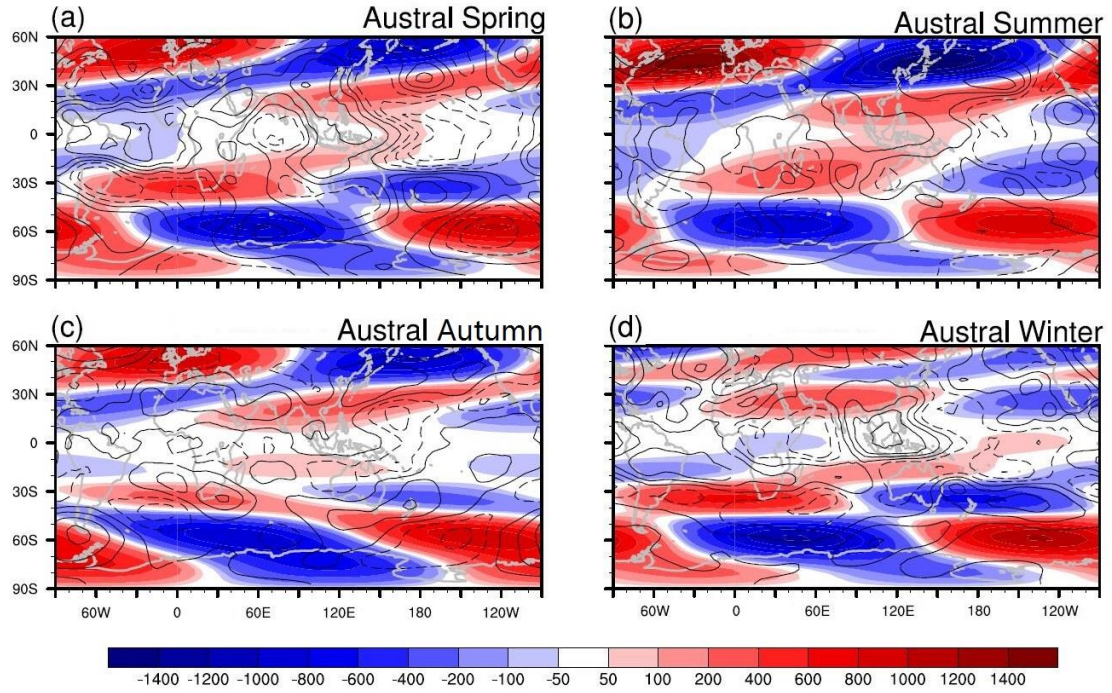


Figure 5. Correlation coefficients (contour level) between the ST_MSEAI and 300-hPa geopotential height associated with stationary waves of wavenumber 1 (color) from the ERA-Interim reanalysis in (a) austral spring, (b) austral summer, (c) austral autumn, and (d) austral winter between 1979 and 2015. Only statistical significance above 95% confidence level is colored. The seasonal cycles and linear trends were removed before calculating the correlation coefficients.

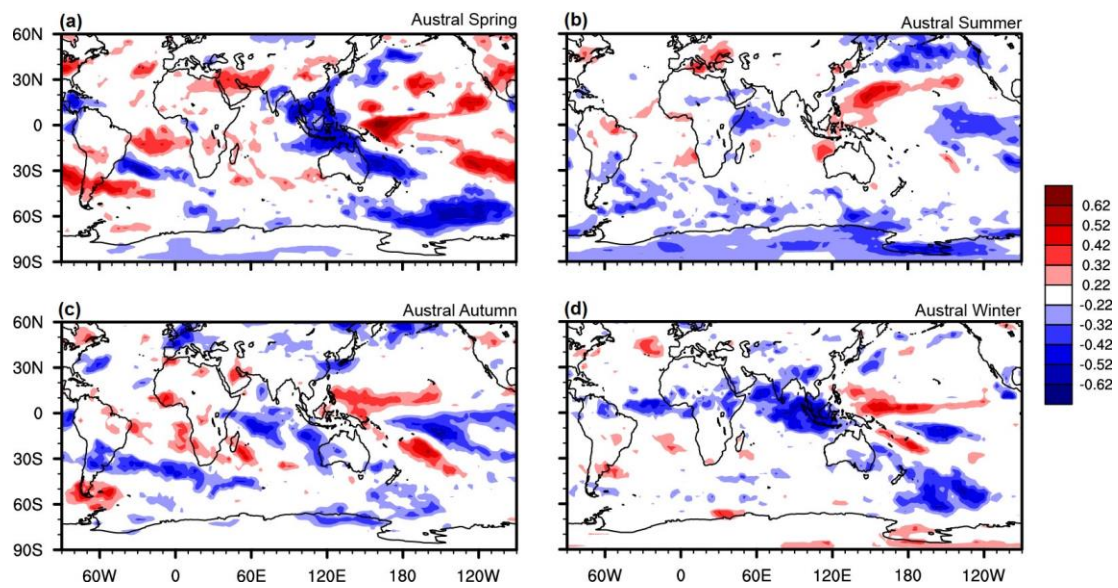


Figure 6. Same as Figure 5, but between the ST_MSEAI and Outgoing longwave radiation from NOAA.

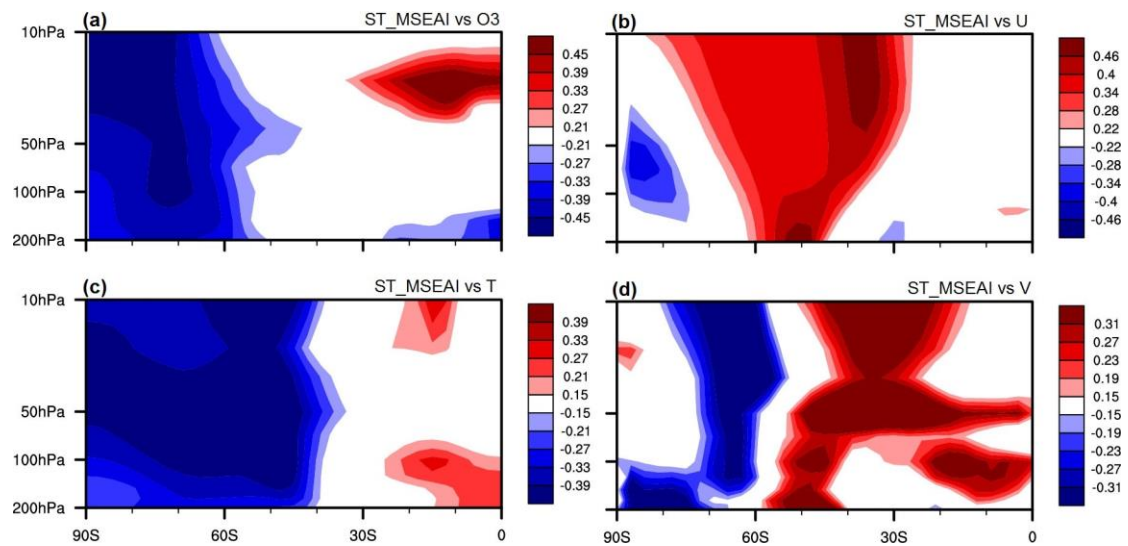
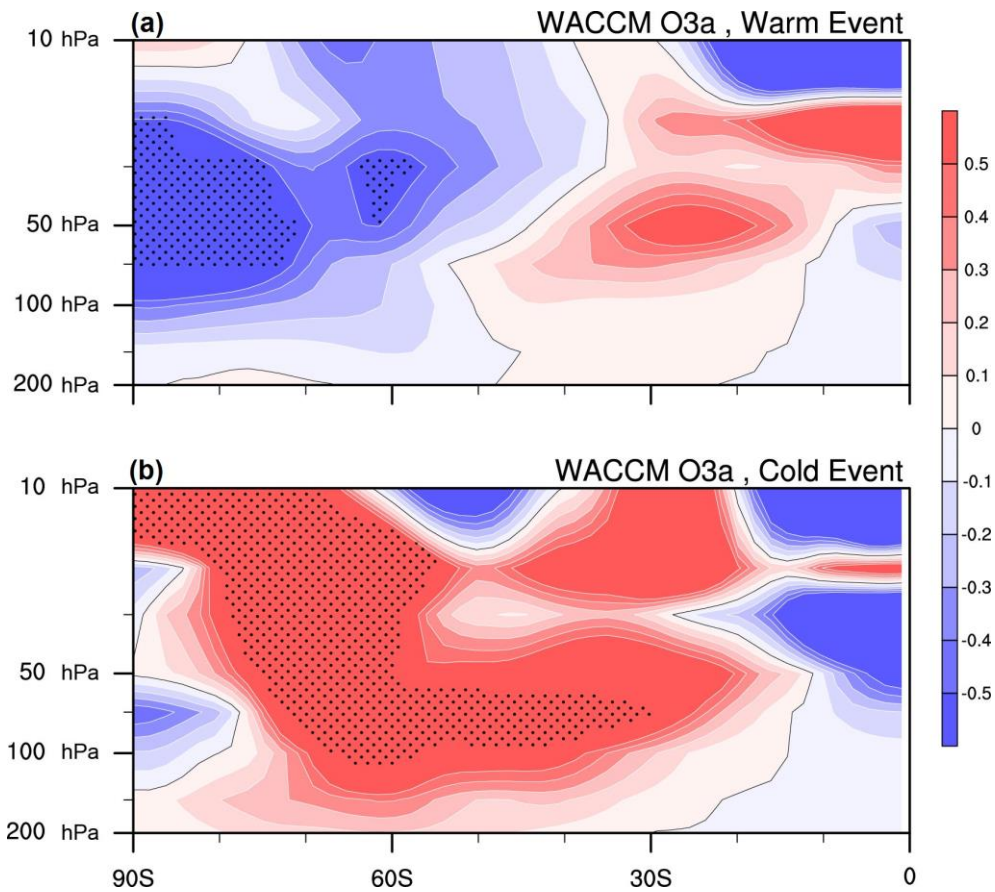


Figure 7. Correlation coefficients between ST_MSEAI and (a) zonally averaged ozone, (b) zonal wind, (c) temperature, and (d) TEM v^* in austral spring (the southward climatological TEM v^* is negative). Wind and temperature from ERA-Interim reanalysis data; ozone from MERRA2. Only statistical significance above 95% confidence level is colored. The seasonal cycles and linear trends were removed before calculating the correlation coefficients.



1
2 **Figure 8.** Zonal mean differences in ozone (ppmv) in austral spring between WACCM simulations
3 (a) S2 and S1, and (b) S3 and S1. Statistical significance above 95% confidence level is stippled.
4 Statistical significance of the simulated anomalies is calculated using the two-tailed Student's
5 t-test.

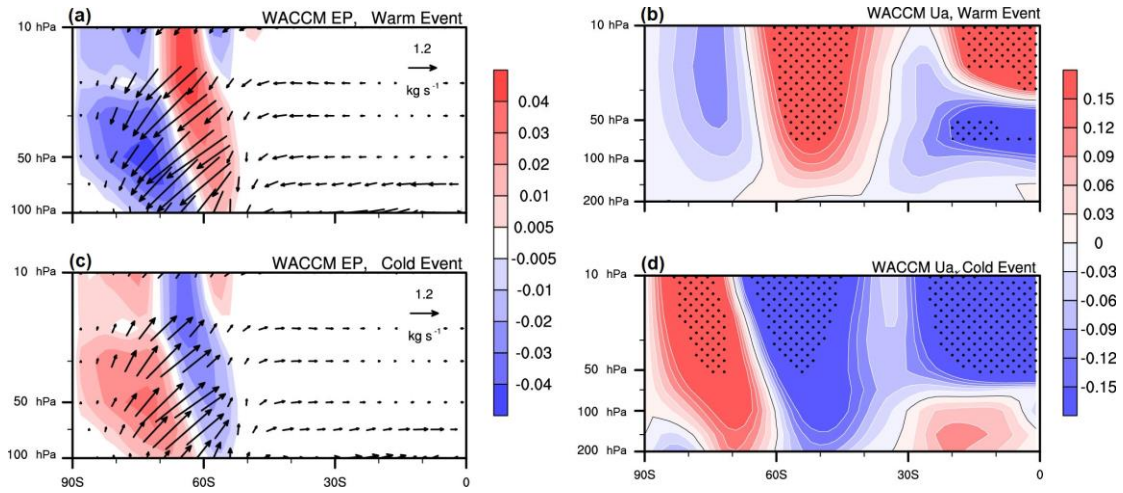


Figure 9. Differences in E–P flux vectors (black arrows) and divergence (color shading) in austral spring between (a) S2 and S1, and (c) S3 and S1. Units for the horizontal and vertical vector directions are 10^7 and 10^5 kg s^{-1} , respectively. (b) and (d), as (a) and (c), but for zonal wind (m s^{-1}). Statistical significance above 95% confidence level is stippled.

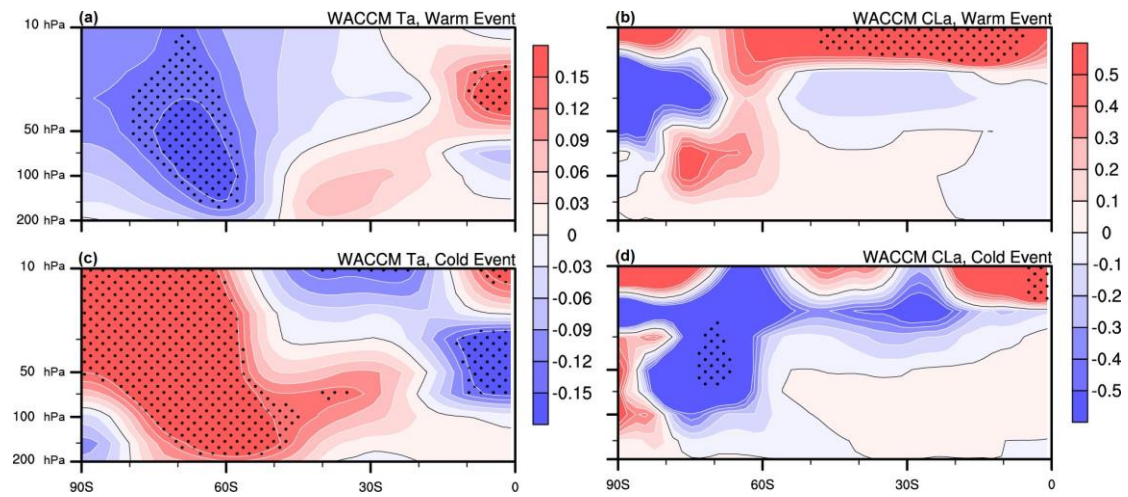
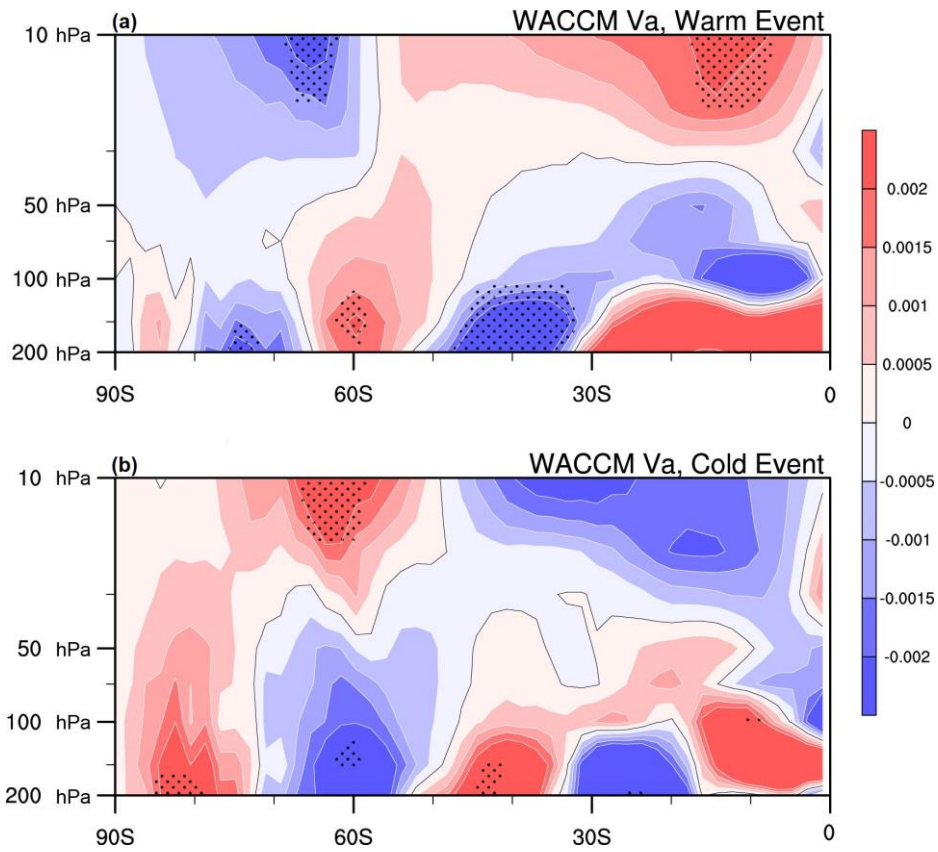


Figure 10. Zonal mean difference in temperature (K) in austral spring between (a) S2 and S1, and (c) S3 and S1. (b) and (d), as (a) and (c), but for active chlorine (ppbv). Statistical significance above 95% confidence level is stippled.

1



2

3 **Figure 11.** Zonal mean difference in TEM meridional wind (m s^{-1}) in austral spring between (a)
 4 S2 and S1, and (b) S3 and S1. Statistical significance above 95% confidence level is stippled.

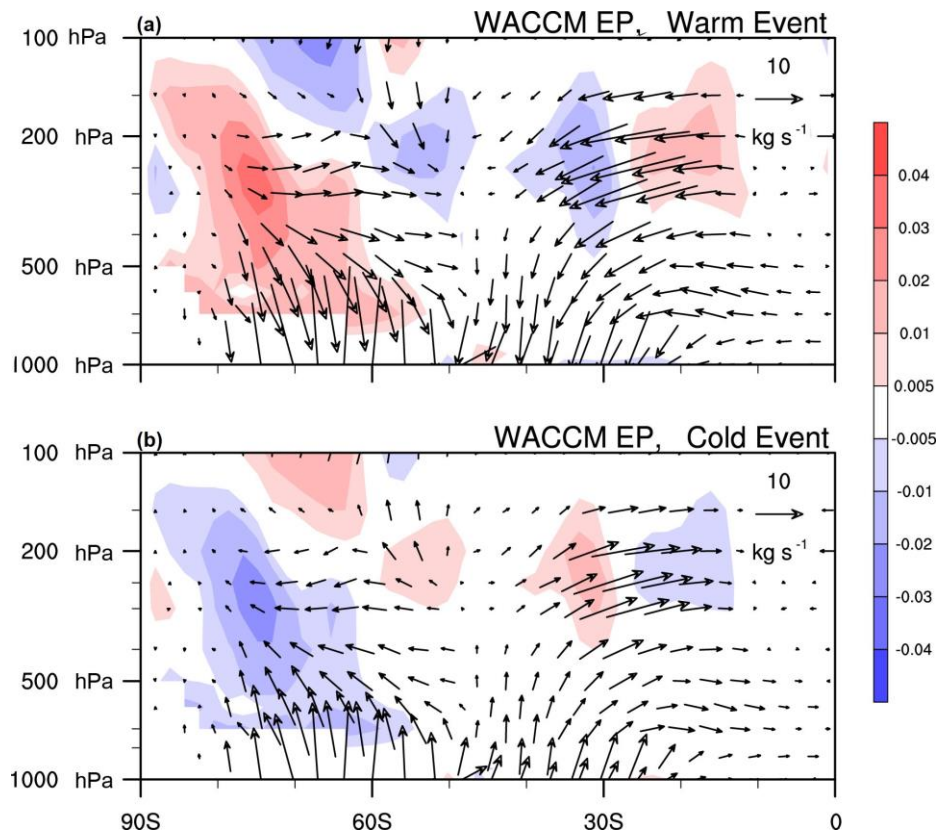


Figure 12. Same as Figure 9a and c, but for 1000 hPa to 100 hPa.

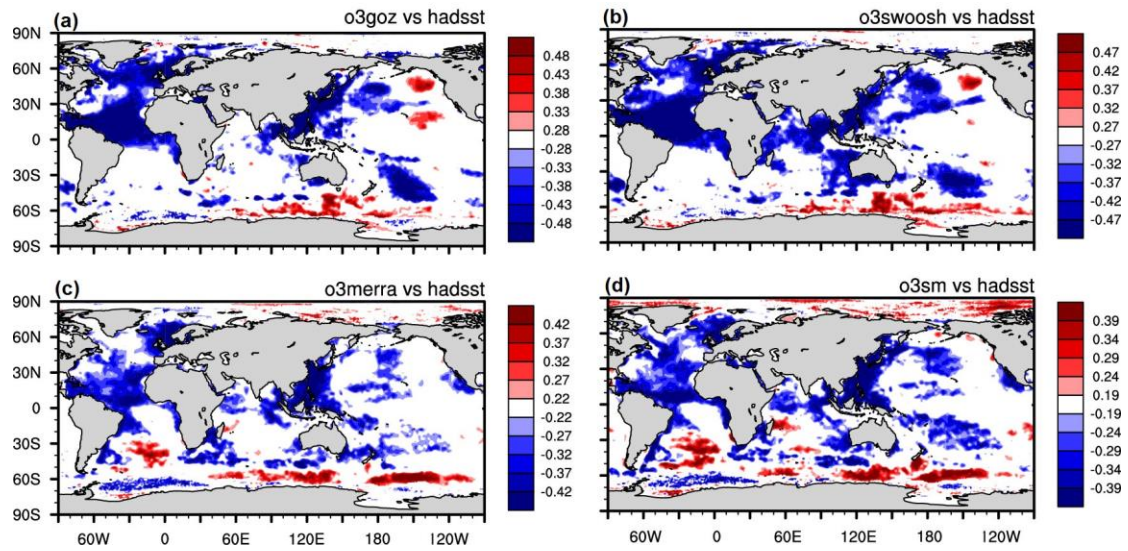
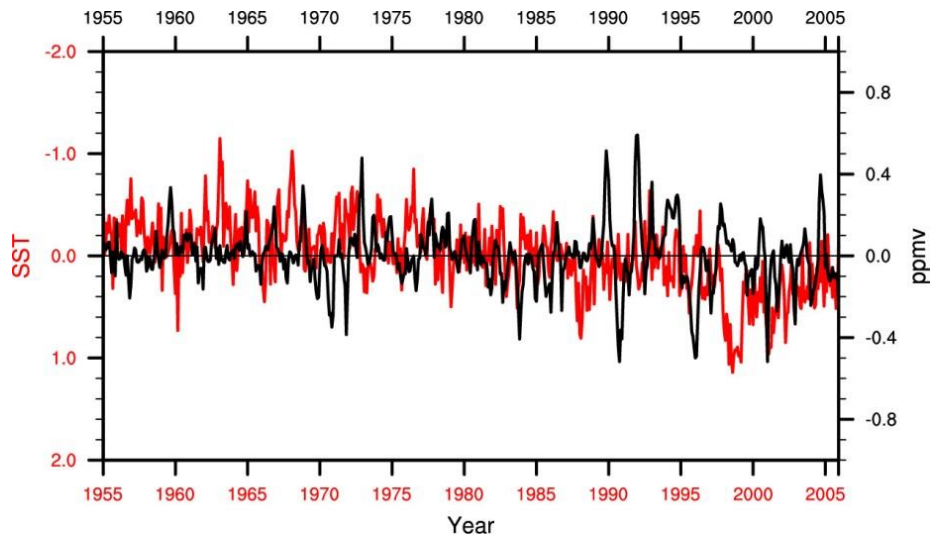


Figure 13. As Fig. 2, but with only the seasonal cycle removed before calculating the correlation coefficients.



1
2 **Figure 14.** The difference in southern high latitude lower stratospheric ozone variations between
3 T1 and $(T2+T3)/2$ (black line) and SST variations in the marginal seas of East Asia (5°S – 35°N ,
4 100°E – 140°E) based on the HadISST data (red line). The seasonal cycle is removed from two
5 time series.